Communications on Applied Nonlinear Analysis
ISSN: 1074-133X
Vol 32 No. 10s (2025)

Resource Allocation in Cognitive Radio 5G Massive MIMO NOMA Systems

Sahar Mohammed Madhloom Al-Inizi[1,2], Mohsen Nickray[1]

[1]Department of computer and information technology, Faculty of engineering Qom University, Qom, Iran.

[2]Najaf technical institute, Al-Furat Al-Awsat Technical University (ATU), Najaf, Iraq.

Corresponding email author: Sahar.mohammed.inj124@atu.edu.iq

Article History:

Received: 12-01-2025

Revised: 15-02-2025

Accepted: 01-03-2025

Abstract:

Mobile telecommunications systems and services are widely deployed across global markets. The proliferation of frequency bands and high-speed services underscores the challenge of managing limited frequency resources in next-generation wireless communication systems. Cognitive radio technology presents a promising solution to efficiently utilize spectrum resources. Additionally, emerging technologies like massive multiple-input-multiple-output (MIMO) and non-orthogonal multiple access (NOMA) enhance spectrum efficiency in these systems. This paper focuses on cluster head selection, user allocation to clusters, and power allocation within clusters in a cognitive radio network employing massive MIMO and power domain NOMA. Cluster head decisions are influenced by primary user interference considerations. User clustering is based on the correlation coefficient between each user's channel correlation matrix and the desired cluster head's spatial vector. Power allocation is formulated as a non-convex optimization problem, simplified for practical implementation using the CVX toolbox in MATLAB. Furthermore, the paper introduces a modified zero-forcing (ZF) beamforming technique that nulls interference toward primary users in downlink connections, demonstrating improved spectrum efficiency compared to conventional interference thresholding methods, as validated through simulation results.

Keywords: Radio Cognitive Networks, Non-orthogonal Multiple Access, Power Allocation, massive MIMO and NOMA Systems, Sum Rate, Convex Optimization, Downlink connection, Spectrum Efficiency, Modified ZF, CVX.

1- Introduction

Cognitive radio (CR) and non-orthogonal multiple access (NOMA) have emerged as significant technologies to improve spectrum efficiency in wireless networks, especially when combined with massive multiple-input multiple-output (MIMO) systems. Zhou et al. [1] provide a comprehensive overview of NOMA's role in cognitive radio networks, detailing the challenges and potential solutions to improve spectrum usage. This review is paralleled by research by Wang and Liu [3], who explore the advancements in cognitive radio networks and suggest that integrating NOMA with these networks could significantly enhance their efficiency. The application of massive MIMO in cognitive radio systems, particularly with NOMA, is considered a transformative approach to address spectrum scarcity. Senel et al. [5] discuss the implications of NOMA in massive MIMO settings, arguing that it could dramatically increase network capacity. Akyildiz et al. [6] provide a broader perspective on next-

generation dynamic spectrum access and cognitive radio networks, underscoring the importance of advanced spectrum sharing techniques to meet the growing demand for wireless communication services. Goldsmith et al. [7] further this discussion by offering an information-theoretic perspective on breaking spectrum gridlock through cognitive radios, which is fundamental in developing strategies for efficient spectrum utilization. Tao et al. [8] survey several technologies of non-orthogonal transmission for 5G, which includes NOMA, indicating its critical role in future wireless networks. Tragos et al. [9] provide a comprehensive survey on spectrum assignment in cognitive radio networks, which is crucial for effective spectrum management and avoiding interference with incumbent users. This is supported by the work of Ding et al. [31], who explore the application of MIMO technologies to NOMA, indicating potential efficiency gains in terms of throughput and user fairness. Resource allocation in these systems is a critical area of study. Higuchi and Benjebbour [13] highlight the efficiency of successive interference cancellation (SIC) in NOMA, which can be crucial for optimizing resource allocation in cognitive radio systems. Further, the work of El Ayach et al. [57] on spatially sparse precoding in millimeter wave MIMO systems points to significant efficiency gains through beamforming techniques, which could be effectively combined with NOMA strategies. Power allocation is another crucial aspect. Shahrokh and Mohamed-pour [2] address sub-optimal power allocation strategies in MIMO-OFDM-based cognitive radio networks, underscoring the trade-offs involved in such systems. Similarly, Zhou et al. [24] and Glei and Chibani [25] discuss the rate-optimal power domain NOMA, emphasizing the need for efficient power allocation to maximize system throughput without causing undue interference to primary users. On the interference management front, Li et al. [32] explore the outage performance of cooperative NOMA networks, emphasizing the need for robust strategies to manage interference in dense network environments. This is crucial in cognitive radio settings where the primary and secondary users must coexist without detrimental interference, as detailed by Proakis [35] in his work on spread spectrum signals for digital communications. The integration of these technologies requires careful consideration of practical limitations and implementation strategies. Srinivasa and Jafar [16] provide a theoretical perspective on the throughput potential of cognitive radios, which could inform practical deployment strategies. Meanwhile, the survey by Islam et al. [23] on power-domain NOMA in 5G systems reviews the potentials and challenges, offering insights into future research directions that could enhance the deployment of cognitive radio massive MIMO NOMA systems. Resource allocation in such integrated systems often requires sophisticated algorithms to handle the dynamic nature of cognitive radio environments. Wang et al. [63] discuss spectrum and energy-efficient beamspace MIMO-NOMA configurations that utilize lens antenna arrays to enhance signal directionality and reception quality. This approach, which strategically allocates resources in millimeter-wave communications, signifies the potential for increased spectrum efficiency and network performance in high-demand scenarios. Furthermore, the need for advanced beamforming techniques, as discussed by El Ayach et al. [57] and Dai et al. [53], is evident in maintaining effective communication in dense network environments where cognitive radios operate. These techniques help manage interference and optimize the spatial distribution of network resources, which are critical for supporting the high data rates required in modern wireless systems. Theoretical studies, such as those by Srinivasa and Jafar [16] and Proakis [35], provide foundational knowledge that aids in understanding the limits and capabilities of these complex systems. Practical implementations, however, must also consider the real-world variabilities

and imperfections that affect system performance. This gap between theoretical potential and practical application is a focal point of ongoing research. The integration of NOMA with cognitive radio-enabled massive MIMO systems also presents unique opportunities for innovation in power allocation strategies. Researchers like Zhou et al. [24] and Glei and Chibani [25] have explored power allocation mechanisms that aim to maximize throughput while adhering to the strict power constraints and interference management requirements of cognitive radios. These studies underscore the delicate balance required between achieving high throughput and maintaining fair access to the spectrum for all users. On the regulatory and standardization front, efforts by Chen et al. [20] and Mohammadi et al. [21] aim to guide the development of frameworks that accommodate the complexities of NOMA in cognitive radio and massive MIMO contexts. These efforts are crucial for ensuring that technological advancements align with global standards and regulations, facilitating wider adoption and interoperability across different networks and regions. Lastly, the evolution of 5G and beyond networks brings additional layers of complexity and opportunity. The work by Sun et al. [52] and Liu et al. [19] on advanced MIMO-NOMA systems and cognitive relaying highlight the ongoing innovation in this space, pushing the boundaries of what is possible in terms of network capacity and efficiency.

A key distinction in conducting this paper compared to other studies is the proposition of an optimal method for resource allocation in a cognitive radio network based on massive MIMO and NOMA technologies. The goal is to maximize network throughput or sum rate in the presence of primary users. This key objective considers the interference introduced by secondary users on the primary user, the total transmitted power constraint in the network, and ensuring the desired SNR for the users. The issue of resource management and efficiency in cognitive radio networks was addressed in Chapter 2, followed by a review of relevant references in the continuation of this chapter. In Chapter 3, focusing on the selected reference, the problem of maximizing the network sum rate along with four constraints was introduced. The objective function of the problem was non-convex and the constraints were linear and convex, based on which we proposed methods to enhance the spectral efficiency and efficiency of the CRMN communication system. Chapter 4 analyzed and examined the results obtained from the simulations conducted based on our proposed methods, comparing the strengths and weaknesses of each method through several graphs. Finally, in the concluding chapter of this paper, we intend to provide a brief summary of the proposed methods and the work carried out in this research.

2- Research background

2-1 Proposed System Model of the Problem

As mentioned in the previous chapter, this chapter of the paper will delve into the investigation of power allocation in a cognitive radio network based on NOMA technology with multiple massive antennas. Reference [66] has been selected as the primary source due to its relevance to the theme of this paper in certain aspects such as NOMA discussion, user clustering, multi-antenna base station, and optimization parameters. Unlike other articles, in articles [53] and [66], the number of users in a NOMA-based system within each cluster is more than 2 users.

As depicted in the following system model, in this cognitive radio network, a cognitive radio base station with multiple antennas, having N transmit antennas serving a primary user and U secondary

users with a single antenna each, based on NOMA and SDMA technologies, and is considered according to the downlink communication state in a cell. Each user occupies a specific spectrum in the available frequency spectrum. The spectral sharing between secondary and primary users is considered in an underlay access pattern. The proposed system model's primary network includes a primary user with a single transmit and receive antenna. The U users are grouped in G clusters ($G<U$). The number of users assigned to cluster g is being considered as N_g.

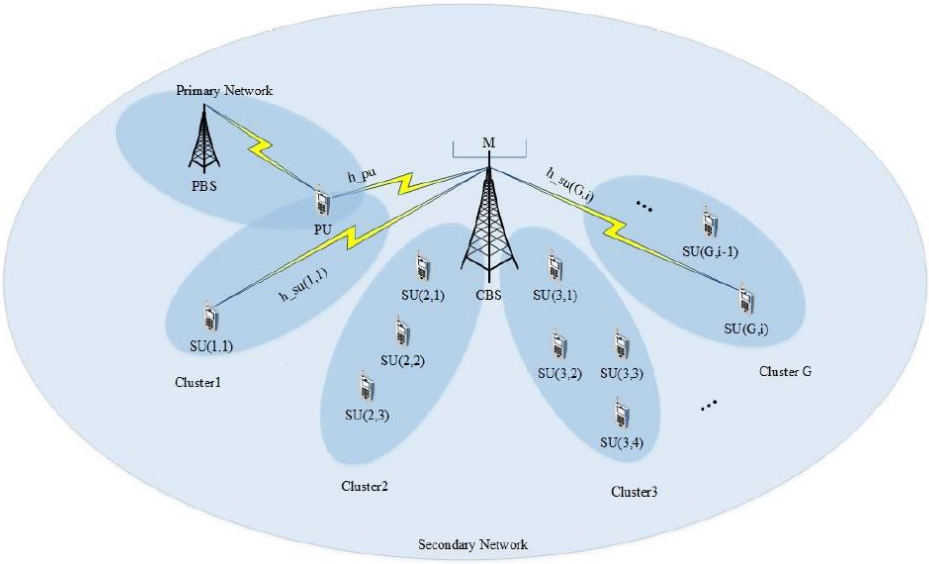

Fig. 3: Proposed CRMN (Cognitive-Radio-MIMO-NOMA) System Model

In the system model shown in Fig. 1-3, the minimum number of users in each cluster is one user, and the number of users in each cluster is different from the number of users in other clusters. On the other hand, due to the fact that the system model is considered to be a massive multi-antenna, our assumption is that the number of CBS transmitting antennas is much more than the number of receiving antennas of all users, so the relationship $N \gg U$ is established.

2-2 Signal Model and Mathematical Relationships

In order to beamforming, the transmitter of a base station employs a Digital Pre-coder when transmitting signals to users. The pre-coding matrix for digital pre-coding is denoted by D. The columns of this matrix are normalized, and its dimensions are $N \times G$, defined as follows:

$$\boldsymbol{D} = [\boldsymbol{d_1}.\boldsymbol{d_2}.\cdots.\boldsymbol{d_G}] \quad (1\text{-}3)$$

In equations (1-3), the normalized digital precoding vector corresponding to cluster (g) is represented as $\boldsymbol{d_g} \in C^{N\times 1}$ and is utilized in the primary user channel and secondary users. The transmitted signal vector from the antennas of the base station is $\boldsymbol{x} \in C^{N\times 1}$ and is formulated as follows:

$$\boldsymbol{x} = \boldsymbol{Ds} \quad (2\text{-}3)$$

The transmitted symbol vector for each cluster, as shown in equation (2-3), $\boldsymbol{s} \in C^{N\times 1}$ is defined as $\boldsymbol{s} = [s_1.s_2.\cdots.s_G]^T$. The transmitted symbols of the primary and secondary users from the base station for

g cluster are denoted as s_g, and the application of the superposition coding scheme in the power domain is as follows:

$$s_{G-SU} = \sum_{m=1}^{N_g} \sqrt{p_{g\cdot m}}\, s_{g\cdot m-SU}$$
$$s_{G-PU} = \sum_{m=1}^{N_g} \sqrt{p_{g\cdot m}}\, s_{g\cdot m-PU} \quad (3\text{-}3)$$

In Eq. (3-3), $p_{g\cdot m}$ represents the power allocated to user m in cluster g, and $s_{g\cdot m}$denotes the message symbol. The transmitted message symbol $s_{g\cdot m}$ is normalized, hence the relation $E\left\{\left|s_{g\cdot m}\right|^2\right\} = 1$ is definitely satisfied..

The information about the channel status between the base station, primary user, and cognitive users for the base station is specified. Therefore, the allocation of power to users by the base station, clustering of users, and beamforming related to clusters can be implemented. If the channel vector between the base station and the *m*-th secondary user in cluster g is defined as $\boldsymbol{h}_{su}$, and the channel vector between the base station and a single primary user in cluster g is defined as $\boldsymbol{h}_{pu}$, the $\boldsymbol{h}_{su}\,.\boldsymbol{h}_{pu}C^{1\times N}$, which represent millimeter-wave MIMO communication channels, are modeled as stated in [57]:

$$\boldsymbol{h_{su}} = \sqrt{\frac{\boldsymbol{N}}{\boldsymbol{L_{g.m}}}} \sum_{\boldsymbol{l=1}}^{\boldsymbol{L_{g.m}}} \boldsymbol{\alpha}_{\boldsymbol{g.m}}^{(\boldsymbol{l})} \cdot \vec{\boldsymbol{\alpha}}_{\boldsymbol{az}} \left(\boldsymbol{\varphi}_{\boldsymbol{g.m}}^{(\boldsymbol{l})}\right)$$
$$\boldsymbol{h_{pu}} = \sqrt{\frac{\boldsymbol{N}}{\boldsymbol{L_{g.m}}}} \sum_{\boldsymbol{l=1}}^{\boldsymbol{L_{g.m}}} \boldsymbol{\alpha}_{\boldsymbol{g.m}}^{(\boldsymbol{l})} \cdot \vec{\boldsymbol{\alpha}}_{\boldsymbol{az}} \left(\boldsymbol{\varphi}_{\boldsymbol{g.m}}^{(\boldsymbol{l})}\right) \quad (4\text{-}3)$$

In Eq. (3-4), the number of paths between the base station and user *m* within cluster g is denoted as $\boldsymbol{L_{g.m}}$. $\boldsymbol{\alpha}_{\boldsymbol{g.m}}^{(\boldsymbol{l})}$ is also a random variable and represents the complex channel coefficient of path *l* where $\boldsymbol{\varphi}_{\boldsymbol{g.m}}^{(\boldsymbol{l})}$is a random variable and azimuth angle of *l* path. On the other hand, $\vec{\boldsymbol{\alpha}}_{\boldsymbol{az}}\left(\boldsymbol{\varphi}_{\boldsymbol{g.m}}^{(\boldsymbol{l})}\right)$ signifies the conductor vector of azimuth angle of antennas arrayed in the direction of user m within cluster g along path *l*. These parameters are also defined for the primary channel, but with the distinction that there is only one primary user. Furthermore, a uniform linear array is used such that it is assumed that all antennas in the array are equally spaced, and the utilization of all N base station antennas in the horizontal direction is in accordance with the following relation [58].

$$\boldsymbol{a}_{az_{(n)}}(\varphi) = \frac{1}{N} exp(j2\pi n(\frac{d}{\lambda})sin(\varphi))$$
$$n = 0.1.2.\cdots.N-1 \quad (5\text{-}3)$$

In Eq. (5-3), d is the horizontal distance between each antenna, λ is the wavelength of the transmitted signal, and $\boldsymbol{a}_{az_{(n)}}(\varphi)$is the n-th element of conductor vector$\vec{\boldsymbol{\alpha}}_{\boldsymbol{az}}\left(\boldsymbol{\varphi}_{\boldsymbol{g.m}}^{(\boldsymbol{l})}\right)$. If the sum of additive white Gaussian noise at the primary user receiver and the *m*-th secondary user in cluster g are v_{su} and v_{pu} respectively, assuming it as a complex circularly symmetric Gaussian noise with variance $\mathcal{CN}(0.\sigma_v^2)$, then the received signal at the *m*-th user receiver in cluster g and the received signal at the primary user in cluster g are as follows:

$$y_{su} = \boldsymbol{h}_{su}^H \boldsymbol{x} + v_{su} = \boldsymbol{h}_{su}^H \boldsymbol{D}\boldsymbol{s} + v_{su} = \boldsymbol{h}_{su}^H \sum_{i=1}^{G}\sum_{j=1}^{N_g} \boldsymbol{d}_i \sqrt{p_{i.j}} s_{i.j} + v_{su}$$
$$y_{pu} = \boldsymbol{h}_{pu}^H \boldsymbol{x} + v_{pu} = \boldsymbol{h}_{pu}^H \boldsymbol{D}\boldsymbol{s} + v_{pu} = \boldsymbol{h}_{pu}^H \sum_{i=1}^{G}\sum_{j=1}^{N_g} \boldsymbol{d}_i \sqrt{p_{i.j}} s_{i.j} + v_{pu} \quad (6\text{-}3)$$

Considering the proposed system, the received signal by each primary and secondary user's receiver can be represented as the desired signal corresponding to the user, intra-cluster interference signal, inter-cluster interference signal, and channel noise. As indicated in Eq. (7-3), the desired signal corresponding to the secondary user m in cluster g, denoted as $s_{g\cdot m-PU}$. Therefore, the remaining signals received by the mentioned user's receiver are considered as interference signals. The key point is to note that the intra-cluster interference signal is the same as the interference signal related to the NOMA scheme. Hence, to combat this type of interference and neutralize its effects, as mentioned in Chapter 1, sequential interference cancellation is utilized by users with stronger channel conditions. This relationship holds for the received signal of the primary user based on its channel conditions as well.

$$y_{g.m-SU} = (\boldsymbol{h}_{su}^H \boldsymbol{d}_{\boldsymbol{g}} \sqrt{p_{g\cdot m}}\, s_{g\cdot m-SU}) + \underbrace{\left(\boldsymbol{h}_{su}^H \boldsymbol{d}_{\boldsymbol{g}} \sum_{\substack{j=1 \\ j\neq m}}^{N_g} \sqrt{p_{g.j}} s_{g.j}\right)}_{\boldsymbol{intra-cluster\ interference\ signa}} + \left(\underbrace{\boldsymbol{h}_{su}^H \boldsymbol{d}_{\boldsymbol{g}} \sum_{\substack{i=1 \\ i\neq g}}^{G}\sum_{j=1}^{N_i} \boldsymbol{d}_{\boldsymbol{i}} \sqrt{p_{i.j}} s_{i.j}}_{\boldsymbol{inter-cluster\ interference\ signa}}\right) + \underbrace{v_{su}}_{channel\ noise} \quad (7\text{-}3)$$

The important and fundamental assumption based on the following relationship is applied to users present in each of the clusters:

$$\left|\boldsymbol{h}_{g.1}^H \boldsymbol{d}_{\boldsymbol{g}}\right| \geq \left|\boldsymbol{h}_{g.2}^H \boldsymbol{d}_{\boldsymbol{g}}\right| \geq \cdots \geq \left|\boldsymbol{h}_{g.N_g}^H \boldsymbol{d}_{\boldsymbol{g}}\right| \quad .g = 1.2.\cdots.G \quad (8\text{-}3)$$

The practical assumption mentioned in relation (8-3) illustrates the process of ordering the primary and secondary user numbers present in a specific cluster based on the channel conditions of users within that cluster. As the user number increases within each cluster, the channel condition of that user in the cluster becomes weaker. In other words, User 1 in each cluster has the strongest channel, and User $N_g$in each cluster has the weakest effective channel. Considering the concepts based on the NOMA scheme mentioned in Chapter 1, users with better channel conditions will have less power allocation, while users with worse channel conditions will have more power allocation. Therefore, for each user belonging to a specific cluster, a user with a weaker channel in that cluster will receive a stronger signal compared to other users in that cluster. In other words, the weakest user in a specific cluster receives their signal stronger than other users in that cluster and therefore only decodes the signal relevant to themselves. It is worth noting that this scenario is only feasible in practice when the difference in power levels between strong user signals and weak user signals in a specific cluster is considerable. Hence, for all *j* falling within the inequality interval $m < j \leq N_g$, the *m*-th user in the *g*-th cluster has the capability to eliminate the interfering signal related to the mentioned users in the *g*-th cluster by employing the SIC method [59].

According to equation (3-9), if $\gamma_{g.m}$ represents the Signal-to-Noise-plus-Interference Ratio (SINR) for user *m* in cluster *g*, then we have:

$$\gamma_{g.m} = \frac{p_{g.m}\left\|\boldsymbol{h}_{g.m}^{H}\boldsymbol{d}_{\boldsymbol{g}}\right\|_2^2}{(\left\|\boldsymbol{h}_{g.m}^{H}\boldsymbol{d}_{\boldsymbol{g}}\right\|_2^2 \sum_{j=1}^{m-1} p_{g.j} + \sum_{\substack{i=1 \\ i\neq g}}^{G}\sum_{j=1}^{N_i} p_{g.j}\left\|\boldsymbol{h}_{g.m}^{H}\boldsymbol{d}_{\boldsymbol{g}}\right\|_2^2 + \sigma_v^2)} \tag{9-3}$$

In Eq. (9-3), for convenience, if we consider the denominator of the fraction to be equal to the scalar quantities $\xi_{g.m}$, we will have:

$$\xi_{g.m} = (\left\|\boldsymbol{h}_{g.m}^{H}\boldsymbol{d}_{\boldsymbol{g}}\right\|_2^2 \sum_{j=1}^{m-1} p_{g.j} + \sum_{\substack{i=1 \\ i\neq g}}^{G}\sum_{j=1}^{N_i} p_{g.j}\left\|\boldsymbol{h}_{g.m}^{H}\boldsymbol{d}_{\boldsymbol{g}}\right\|_2^2 + \sigma_v^2) \tag{10-3}$$

According to Shannon's equation, the maximum achievable information rate accessible to the *m*-th secondary user in cluster *g*, considering BW as the system's communication bandwidth, will be calculated as follows:

$$R_{g.m} = BW \times log_2(1 + \gamma_{g.m}) \tag{11-3}$$

Therefore, the total achievable sum rate for all users in the system is calculated as the following equation:

$$R_{sum} = \sum_{g=1}^{G}\sum_{m=1}^{N_g} R_{g.m} \tag{12-3}$$

Moreover, the system spectral efficiency will also be obtained according to the following relationship:

$$SE = \frac{R_{sum}}{BW} \tag{13-3}$$

According to Eq. (13-3), in order to enhance the spectral efficiency of the system, efficient user clustering, effective pre-coding for each cluster, and optimal power allocation of NOMA to each user must be utilized. As we know, it is very challenging to simultaneously obtain the optimal method and solution for each of the parameters mentioned above. In the following, we will thoroughly investigate the optimization problem for NOMA power allocation in the proposed CRMN network.

The summary of our work process is as follows: Initially, we incorporate cognitive radio interference constraints by defining a threshold from the primary user side to the issue so that the base station, managed by power control, can manage incoming interferences from secondary users to primary users. Subsequently, we propose a method for selecting clusters in cognitive radio networks, and finally, an amended beamforming method is introduced as an alternate approach.

3- Proposed Method

The primary goal of next-generation telecommunications systems is to achieve high-quality services for all users in the network, each requiring its own specific strategies. Resource allocation aiming to maximize the total sum rate of all users with NOMA power optimization variable is formulated as a $\boldsymbol{P_1}$ problem:

$$\boldsymbol{P_1}: \begin{cases} \max\limits_{\{p_{g.m}\}} \sum\limits_{g=1}^{G} \sum\limits_{m=1}^{N_g} R_{g.m} \\ \boldsymbol{Susbject\ to.} \quad C_1^{(p_1)}: p_{g.m} \geq 0 \ . \quad \forall g.m \\ C_2^{(p_1)}: \sum\limits_{g=1}^{G} \sum\limits_{m=1}^{N_g} p_{g.m} \leq P_{max} \\ C_3^{(p_1)}: p_{g.m+1} \geq \alpha \times p_{g.m} \ . \quad \forall g.m \end{cases}$$

In problem $\boldsymbol{P_1}$, $R_{g.m}$ represents an argument of the objective function, essentially indicating the maximum achievable throughput of the cognitive radio network and the achievable rate of information by user m in cluster g. The optimization variable $\{p_{g.m}\}$is the power allocated by the NOMA scheme to users in each cluster, thereby maximizing the objective function. The parameters P_{max}, α, and $I_{th}$are known as inputs to the problem, representing respectively the maximum power from the transmitter's power amplifier, the Scale Ratio factor greater than 1 , and the maximum tolerable interference level for the primary user. The constraint $C_1^{(p_1)}$is a non-negativity constraint on the power allocated by each user for each m, g. The constraint $C_2^{(p_1)}$limits the power level that can be transmitted by the base station or, in other words, at best, it corresponds to the total power allocated to all users, which is equivalent to the power transmitted by the base station. The constraint $C_3^{(p_1)}$ defines the power allocation among users close and far from the base station in all clusters. By satisfying this constraint, fairness in the allocation of power levels to weak and strong users is ensured, the SIC method is correctly implemented in the user receivers, and severe SINR degradation for weak users is prevented. By imposing this constraint, the problem of power allocation among users within each cluster in the reference [53], which was in conflict with the nature of NOMA, was corrected [66]. By generalizing the issue to the cognitive radio domain, one of the most significant challenges we will face is the

interferences affecting the primary user. Hence, the proposed methods discussed below are considered as solutions for minimizing these interferences. Continuing, we define the optimization problem $\boldsymbol{P_2}$. We introduce the proposed methods in each subsection and then formulate the problem for optimizing the total system rate of the proposed system.

3-1 First Proposed Method: Power Management by Interference Threshold Setting in CRMN System

Problem $\boldsymbol{P_2}$is an optimization problem of resource allocation in the CRMN system, with the objective function of maximizing the sum rate of cognitive radio network. The constraints of problem $\boldsymbol{P_2}$include total transmit power of cognitive radio network, power allocation for ensuring fairness among users with different channel conditions, and the interference constraint introduced by secondary users on primary users. Ultimately, the problem is formulated to optimize NOMA power as follows:

$$\boldsymbol{P_2}:\begin{cases} \max\limits_{\{p_{g.m}\}} \sum\limits_{g=1}^{G}\sum\limits_{m=1}^{N_g} R_{g.m} \\ \boldsymbol{Susbject\ to}. \quad C_1^{(p_2)}: p_{g.m} \geq 0 \ . \quad \forall g.m \\ C_2^{(p_2)}: \sum\limits_{g=1}^{G}\sum\limits_{m=1}^{N_g} p_{g.m} \leq P_{max} \\ C_3^{(p_2)}: p_{g.m+1} \geq \alpha \times p_{g.m} \ . \quad \forall g.m \\ C_4^{(p_2)}: \sum\limits_{g=1}^{G}[\left\|\boldsymbol{h_{pu}}\boldsymbol{d_g}\right\|_2^2 \sum\limits_{m=1}^{N_g} p_{g.m}] \leq I_{th} \ . \quad \forall g.m \end{cases}$$

The difference between the optimization problem $\boldsymbol{P_1}$and the problem $\boldsymbol{P_2}$lies in the addition of a constraint $C_4^{(p_2)}$that represents the interference constraint imposed by cognitive radio users on the primary user; since no interference should occur for the primary user when using the channel, the base station should control interference by reducing its power to a level below the interference threshold that is tolerable for the primary user and prevent interference on the PU channel. The objective function of problem $\boldsymbol{P_1}$, as indicated by the definition of sum rate and Shannon's Law in Eq. (11-3), is a logarithmic function and essentially a non-convex optimization problem with respect to the optimization variables $\{p_{g.m}\}$ that satisfy convexity conditions; all constraints of the problem are linear and convex. The subscription of four $\boldsymbol{P_1}$problem constraints forms a convex feasible set, hence for a problem to be convex with linear constraints, the objective function must be convex. Therefore, by simplifications and utilizing several lemmas, a convex optimization problem can be transformed into one, and ultimately, its decomposition and analysis are conducted in MATLAB software using the CVX toolbox. This toolbox is highly practical and important for solving complex convex optimization problems effectively. It is essential to note that before using the CVX toolbox, the problem must be transformed into a standard Disciplined Convex Programming in order to be definable for this toolbox. According to interpretations, we need to address the simplification of the optimization problem $\boldsymbol{P_2}$; to this end, we first introduce the following lemma.

Lemma 1: Considering the Sherman-Morrison-Woodbury matrix relation [60]:

$$(\mathbf{A}+\mathbf{BCD})^{-1}=\mathbf{A}^{-1}-\mathbf{A}^{-1}\mathbf{B}(\mathbf{I}+\mathbf{CDA}^{-1}\mathbf{B})^{-1}\mathbf{CDA}^{-1} \quad (14\text{-}3)$$

Given the relationships (3-9) and (3-10), we have the following equation:

$$\gamma_{g.m}=\frac{p_{g.m}\left\|\boldsymbol{h}_{g.m}^{H}\boldsymbol{d}_{\boldsymbol{g}}\right\|_2^2}{\xi_{g.m}}=p_{g.m}\left\|\boldsymbol{h}_{g.m}^{H}\boldsymbol{d}_{\boldsymbol{g}}\right\|_2^2\xi_{g.m}^{-1} \quad (15\text{-}3)$$

Based on relation (3-15) and using **Lemma 1**, the following relation is established:

$$(1+\gamma_{g.m})^{-1}=1-p_{g.m}\left\|\boldsymbol{h}_{g.m}^{H}\boldsymbol{d}_{\boldsymbol{g}}\right\|_2^2\left(p_{g.m}\left\|\boldsymbol{h}_{g.m}^{H}\boldsymbol{d}_{\boldsymbol{g}}\right\|_2^2+\xi_{g.m}\right)^{-1} \quad (16\text{-}3)$$

On the other hand, for the sake of simplicity, relation (3-17) can be rewritten as follows:

$$\tilde{y}_{g.m-SU}=\boldsymbol{h}_{su}^{H}\boldsymbol{d}_{\boldsymbol{g}}\sqrt{p_{g.m}}s_{g.m-SU}+\boldsymbol{h}_{su}^{H}\boldsymbol{d}_{\boldsymbol{g}}\sum_{j=1}^{m-1}\sqrt{p_{g.j}}s_{g.j} \quad (17\text{-}3)$$

$$+\boldsymbol{h}_{su}^{H}\sum_{\substack{i=1\\ i\neq g}}^{G}\sum_{j=1}^{N_i}\boldsymbol{d}_{\boldsymbol{g}}\sqrt{p_{g.j}}s_{g.j}+v_{g.m}$$

If the Minimum Mean Square Error (MMSE) method is employed by user *m*'s receiver in cluster *g* for detecting the desired signal $s_{g.m}$, which corresponds to user *m* in cluster *g*, then the Mean Squared Error is defined as follows:

$$e_{g.m}=E\{\left|s_{g.m}-c_{g.m}\tilde{y}_{g.m}\right|^2\} \quad (18\text{-}3)$$

$c_{g.m}$is the Channel Equalization Coefficient in equation (3-18), and its optimal value is calculated as follows:

$$c_{g.m}^{opt}=arg\min_{c_{g.m}}e_{g.m} \quad (19\text{-}3)$$

By substituting equation (3-17) into equation (3-18), we will have:

$$e_{g.m}=1-2Re\{c_{g.m}\sqrt{p_{g.m}}\boldsymbol{h}_{g.m}^{H}\boldsymbol{d}_{\boldsymbol{g}}\}+\left|c_{g.m}\right|^2\left(p_{g.m}\left\|\boldsymbol{h}_{g.m}^{H}\boldsymbol{d}_{\boldsymbol{g}}\right\|_2^2+\xi_{g.m}\right) \quad (20\text{-}3)$$

Based on the principles of optimization, in order to minimize the objective function with respect to the optimal unknown variable optimization, we must take the partial derivative of the objective function $e_{g.m}$ with respect to the unknown variable $c_{g.m}$, and set the resulting partial derivative equal to zero to find the optimal value of $c_{g.m}$ that minimizes the objective function.

After this step, according to equations (3-19) and (3-20), the optimal value of the channel equalization coefficient will be obtained as follows:

$$c_{g.m}^{opt}=(\sqrt{p_{g.m}}\boldsymbol{h}_{g.m}^{H}\boldsymbol{d}_{\boldsymbol{g}})\left(p_{g.m}\left\|\boldsymbol{h}_{g.m}^{H}\boldsymbol{d}_{\boldsymbol{g}}\right\|_2^2+\xi_{g.m}\right)^{-1} \quad (21\text{-}3)$$

Then by substituting Equation (3-21) into Equation (3-20), the optimal value of the least squares mean error is calculated as follows:

$$e_{g.m}^{opt} = 1 - (p_{g.m}\left\|\boldsymbol{h}_{g.m}^{H}\boldsymbol{d}_{\boldsymbol{g}}\right\|_2^2)(p_{g.m}\left\|\boldsymbol{h}_{g.m}^{H}\boldsymbol{d}_{\boldsymbol{g}}\right\|_2^2 + \xi_{g.m})^{-1} \quad (22\text{-}3)$$

Where Equation (3-21) is equivalent to Equation (3-16), therefore we have:

$$(1 + \gamma_{g.m})^{-1} = \min_{c_{g.m}} e_{g.m} \quad (23\text{-}3)$$

After substituting Equation (3-23) into Equation (3-11) assuming $BW = 1Hz$, Equation (3-11) is rewritten as follows:

$$R_{g.m} = log_2\big((1 + \gamma_{g.m}\big) = -log_2\left(\min_{c_{g.m}} e_{g.m}\right) = \min_{c_{g.m}}(-log_2 e_{g.m}) \quad (24\text{-}3)$$

To simplify Equation (3-24), we introduce a new lemma.

Lemma 2: We consider the following assumption [61]:

$$f(a) - \frac{ab}{ln2} + log_2(a) + \frac{1}{ln2} \quad (25\text{-}3)$$

If the optimal value of a is in the form of $a^{opt} = \frac{1}{b}$, then for $a > 0$, the following relationship holds true:

$$\max_{a} f(a) = -\, log_2(ab) \quad (26\text{-}3)$$

Based on Lemma 2, Equation (3-24) is rewritten as follows:

$$R_{g.m} = \max_{c_{g.m}} \max_{c_{g.m}>0} (-\frac{a_{g.m}e_{g.m}}{ln2} + log_2\big(a_{g.m}\big) + \frac{1}{ln2} \quad (27\text{-}3)$$

Where $a_{g.m}$in Equation (3-27) is calculated as follows:

$$a_{g.m} = \frac{1}{e_{g.m}^{opt}} = \frac{1}{1 - (1 - (p_{g.m}\left\|\boldsymbol{h}_{g.m}^{H}\boldsymbol{d}_{\boldsymbol{g}}\right\|_2^2)(p_{g.m}\left\|\boldsymbol{h}_{g.m}^{H}\boldsymbol{d}_{\boldsymbol{g}}\right\|_2^2 + \xi_{g.m})^{-1})} \quad (28\text{-}3)$$

By substituting equation (3-27) into the optimization problem $\boldsymbol{P_2}$, since the value $\frac{1}{ln2}$is a constant numerical value, it is therefore irrelevant in the analysis of the optimization problem and we can exclude it from the objective function argument. Subsequently, the optimization problem $\boldsymbol{P_2}$ is transformed into a new optimization problem $\boldsymbol{P_3}$ and formulated as follows:

$$\boldsymbol{P_3}: \begin{cases} \max\limits_{\{p_{g.m}\}} \sum\limits_{g=1}^{G}\sum\limits_{m=1}^{N_g} \max\limits_{c_{g.m}} \max\limits_{c_{g.m}>0} (-\frac{a_{g.m}e_{g.m}}{ln2} + log_2\big(a_{g.m}\big)) \\ \quad \boldsymbol{Susbject\ to}. \quad C_1^{(p_3)}: p_{g.m} \geq 0 \ . \quad \forall g.m \\ \quad C_2^{(p_3)}: \sum\limits_{g=1}^{G}\sum\limits_{m=1}^{N_g} p_{g.m} \leq P_{max} \\ \quad C_3^{(p_3)}: p_{g.m+1} \geq \alpha \times p_{g.m} \ . \quad \forall g.m \\ \quad C_4^{(p_3)}: \sum\limits_{g=1}^{G}[\left\|\boldsymbol{h}_{\boldsymbol{pu}}\boldsymbol{d}_{\boldsymbol{g}}\right\|_2^2 \sum\limits_{m=1}^{N_g} p_{g.m}] \leq I_{th} \ . \quad \forall g.m \end{cases}$$

Based on the optimization problem formulation $\boldsymbol{P_3}$, first the problem needs to be related to the variables $\{c_{g.m}\}$and $\{a_{g.m}\}$. Then, the problem should be optimized with respect to the optimal values of these variables relative to the variable $\{p_{g.m}\}$, while according to equations (21-3) and (3-28), both variables $\{c_{g.m}\}$and $\{a_{g.m}\}$ are dependent on the values of the variable $\{p_{g.m}\}$. An iterative optimization algorithm is employed to analyze the $\boldsymbol{P_3}$ problem, in which the variable $\{p_{g.m}\}$ is optimized and then subsequently, the variables $\{c_{g.m}\}$and $\{a_{g.m}\}$ are optimized together simultaneously. The details of this process are described as pseudo code in the following algorithm.

Algorithm for calculating the combination of $c_{g.m}$and $a_{g.m}$according to the values of $p_{g.m}$in the previous iteration

The known inputs of the algorithm

t:$Number\ of\ algorithm\ iteration$

$Counter$:$Number\ of\ CVX\ Toolbox\ Executing$

$p_{g.m}^{(0)}$: $Initial\ value\ for\ p_{g.m}$

ε: $Convergence\ Parameter$

$t = 1 \quad .p_{g.m}^{(0)} = \frac{P_{max}}{U} \ . \qquad \varepsilon = 10^{-5}$

Algorithm implementation steps

1- While $t < Counter \qquad \left|p_{g.m}^{(t)} - p_{g.m}^{(t-1)}\right| > \varepsilon$

2- Compute optimal value of $p_{g.m}^{(t)}$ by CVX Toolbox based on Problem $\boldsymbol{P_3}$

3- t= t+1

4- Update value of $c_{g.m}^{(t)}$ & $a_{g.m}^{(t)}$ based on Problem $\boldsymbol{P_3}$

5- End **While**

Termination of the algorithm

In order to clarify the matter, it is assumed that according to the optimal values obtained for the variables $\{p_{g.m}\}$in iteration t-1 of the algorithm, the optimal values of the variables $\{c_{g.m}\}$and $\{a_{g.m}\}$ in the *t*-th iteration of this algorithm will be calculated as follows:

$$c_{g.m}^{(t)} = \left(\sqrt{p_{g.m}^{(t-1)}}\, \boldsymbol{h}_{g.m}^{H} \boldsymbol{d_g}\right) (p_{g.m}^{(t-1)} \left\|\boldsymbol{h}_{g.m}^{H} \boldsymbol{d_g}\right\|_2^2 + \xi_{g.m}^{(t-1)})^{-1} \qquad (29\text{-}3)$$

$$a_{g.m}^{(t)} = \frac{1}{e_{g.m}^{opt(t)}} \tag{30-3}$$

In equations (3-29) and (3-30), the variables $\xi_{g.m}^{(t-1)}$ and $e_{g.m}^{opt(t)}$ are calculated as follows:

$$\xi_{g.m}^{(t-1)} = \left\|\boldsymbol{h}_{g.m}^{H}\boldsymbol{d_g}\right\|_2^2 \sum_{j=1}^{m-1} p_{g.j}^{(t-1)} + \sum_{\substack{i=1 \\ i\neq g}}^{G}\sum_{j=1}^{N_i} p_{g.j}^{(t-1)}\left\|\boldsymbol{h}_{g.m}^{H}\boldsymbol{d_g}\right\|_2^2 + \sigma_v^2 \tag{31-3}$$

$$e_{g.m}^{opt(t)} = 1 - (p_{g.m}^{(t-1)}\left\|\boldsymbol{h}_{g.m}^{H}\boldsymbol{d_g}\right\|_2^2)(p_{g.m}^{(t-1)}\left\|\boldsymbol{h}_{g.m}^{H}\boldsymbol{d_g}\right\|_2^2 + \xi_{g.m}^{(t-1)})^{-1} \tag{32-3}$$

Moreover, $e_{g.m}$ is considered as one of the arguments of the objective function of the optimization problem $\boldsymbol{P_3}$. The optimal values calculated for the variable $p_{g.m}$ in the t-1 iteration of the above algorithm are dependent, and in the t iteration of the algorithm, calculations are written as:

$$e_{g.m}^{(t)} = 1 - 2Re\left\{c_{g.m}^{(t)}\sqrt{p_{g.m}^{(t)}}\boldsymbol{h}_{g.m}^{H}\boldsymbol{d_g}\right\} + \left|c_{g.m}^{(t)}\right|^2(p_{g.m}^{(t)}\left\|\boldsymbol{h}_{g.m}^{H}\boldsymbol{d_g}\right\|_2^2 + \xi_{g.m}^{(t)}) \tag{33-3}$$

After the insertion of relation (3-10) into relation (3-33), we will have:

$$\begin{aligned}\tilde{e}_{g.m}^{(t)} &= 1 - 2Re\left\{c_{g.m}^{(t)}\boldsymbol{h}_{g.m}^{H}\boldsymbol{d_g}\right\}\sqrt{p_{g.m}^{(t)}} \\ &+\left|c_{g.m}^{(t)}\right|^2(\left\|\boldsymbol{h}_{g.m}^{H}\boldsymbol{d_g}\right\|_2^2\sum_{j=1}^{m} p_{g.j}^{(t)} + \sum_{\substack{i=1 \\ i\neq g}}^{G}\sum_{j=1}^{N_i} p_{g.j}^{(t)}\left\|\boldsymbol{h}_{g.m}^{H}\boldsymbol{d_g}\right\|_2^2 + \sigma_v^2\end{aligned} \tag{34-3}$$

In the end, the objective function of relation (3-35) is a convex function:

$$\min_{\{p_{g.m}^{(t)}\}} = \sum_{g=1}^{G}\sum_{m=1}^{N_g} a_{g.m}^{(t)}\,\tilde{e}_{g.m}^{(t)} \tag{35-3}$$

Using the objective function relationship (3-53), the new problem $\boldsymbol{P_4}$ is a convex standard optimization problem because it has a convex objective function and four convex constraints, all of which jointly form a convex feasible region for the problem. The convex optimization formulation of problem $\boldsymbol{P_4}$ is as follows:

By convexifying the $\boldsymbol{P_4}$optimization problem to its standard form in the MATLAB simulation software, this problem can be defined in the CVX toolbox and solved using numerical analysis methods. The objective function of this problem is expected to reach its minimum value due to the interference nature of the signal types through optimization. The variable $p_{g.m}$, representing the power allocation factor for the NOMA scheme in cognitive radio networks, is optimized through simulating this complex problem in the CVX toolbox, yielding the output of the $\boldsymbol{P_4}$optimization problem. By implementing this method, the interference caused by secondary users on the primary user channel is significantly mitigated. This is achieved by reducing and controlling the power of secondary users to meet the threshold I_{th} set by the primary user, thereby managing the interferences. Consequently, with

the desirable conditions in the primary user channel, the primary user will receive the signal with minimal interference at their receiver. All results will be detailed, interpreted, and evaluated in the form of figures and graphs in Chapter Four.

$$\boldsymbol{P_4}: \begin{cases} \max\limits_{\{p_{g.m}^{(t)}\}} \sum\limits_{g=1}^{G} \sum\limits_{m=1}^{N_g} a_{g.m}^{(t)}\, \tilde{e}_{g.m}^{(t)} \\ \textbf{Susbject to}. \quad C_1^{(p_3)}: p_{g.m} \geq 0 \ . \quad \forall g.m \\ C_2^{(p_3)}: \sum\limits_{g=1}^{G} \sum\limits_{m=1}^{N_g} p_{g.m} \leq P_{max} \\ C_3^{(p_3)}: p_{g.m+1} \geq \alpha \times p_{g.m} \ . \quad \forall g.m \\ C_4^{(p_3)}: \sum\limits_{g=1}^{G} [\left\| \boldsymbol{h_{pu} d_g} \right\|_2^2 \sum\limits_{m=1}^{N_g} p_{g.m}] \leq I_{th} \ . \quad \forall g.m \end{cases}$$

3-2 Second Proposed Method: Choosing Cluster Heads Considering Initial User Status

To initiate user clustering, it is necessary to designate one user as the cluster head for each cluster. The objective of this task is to align the beam forming direction of the array of transmitter antennas of the Base Station towards the cluster head of each cluster. In the previous sections, we discussed the CHS algorithm for selecting cluster heads. According to this algorithm, user clustering is achieved based on the correlation between the channels of the remaining users and the cluster heads. A cognitive radio network consists of a number of secondary users and one primary user; therefore, in the context of selecting cluster heads, attention must be paid to the fact that the remaining users who are around the Primary User (PU) and meet the criteria for becoming cluster heads should not be chosen as cluster heads in order to have the least impact on the PU. As mentioned in the user clustering section, to avoid problem complexity, we assign only one beam to each cluster. Since we use ZF beamforming method, if a user present around the initial user is selected as the master user, the beam direction focuses towards that user, allowing them to receive significant benefits from the antenna array. Consequently, the received signal becomes very strong, enabling a substantial decrease in antenna array utilization towards the initial user to prevent interference within the master user cluster. Therefore, we should consider this approach as another proposed method in the context of investigating the correlation of the master channel with other lingering cognitive users. By implementing this technique, when calculating the correlation of users with master clusters, we introduce a new factor to reduce the impact of other cognitive users on the Primary User (PU). Furthermore, based on the favorable outcomes of utilizing special channel matrix values as referenced in [62], when assigning users to each cluster, we consider the coefficient of correlation between the eigenvector corresponding to the largest eigenvalue of the channel matrix and the correlation of each user's channel with the target master cluster. This approach is employed in Algorithm 1 as described below. All inputs of the algorithm must be specified, such as the number of users in the system, the channel vector of each user, the number of clusters for user clustering, and the initial adaptive threshold value, denoted as *T*. Additionally, *Set* represents the set of users selected as cluster heads, and Set^c denotes the set of users that are candidates for cluster

head selection at each stage. The algorithm iterates until cluster heads are determined for all clusters, meaning the number of iterations is proportional to the number of clusters considered. Ultimately, in the algorithm output, we have a number of users equal to the number of clusters selected as cluster headsets for the proposed CRMN network. It is worth mentioning again that at each stage the proposed algorithm is executed, the degree of correlation between each user's channel and the channels of cluster heads selected in the previous stage is determined by calculating the inner product of their normalized channel vectors.

Algorithm 1: Selecting the cluster head for all clusters with the least impact on PU in the CRMN system

The inputs of the algorithm

Number of Users = K, Number of Clusters = G;

User Channel Vector=$\boldsymbol{h}_k$, $k = 1\ .2\ .\ldots.\ K$;

Initial Threshold = T= 0 , $Primary\ user\ channel\ coefficient$=$\beta$=0.5

Algorithm implementation steps

$Clusters\ Head\ Set$: Set

1- $a_k = \|h_k\|_2$; % users channel vector's 2-norm

2- $A = [\ a_1\ , a_2\ , \ldots , a_K\ ]$;

3- $\tilde{h}_k = h_k / a_k$; % secondary users channel vector's normalization

4- $A_{sort} = sort\ (\ A\ , '\ descend\ '\ )$; % users ordering from strong to weak

5- Set=A_{sort} (1);

6- $Set^c = A_{sort}\ /\ \Gamma$;

7- $\Omega =\ \Phi$;

8- g=2;

9- **while** $g \leq G$

10- **if** $\Omega\ ==\ \Phi$

11- **while** $\Omega\ ==\ \Phi$

12- $T\ =\ T\ + \frac{1-T}{10}$; % increase adaptive threshold level

13- $\Omega = \{\ i\ \in\ Set^c\ |\left|\boldsymbol{eigvec}\ \boldsymbol{h}_i^{\boldsymbol{H}}.\boldsymbol{eigvec}\ \boldsymbol{h}_j\right| + \boldsymbol{\beta}\left|\tilde{\boldsymbol{h}}_i^{\boldsymbol{H}}\tilde{\boldsymbol{h}}_{\boldsymbol{pu}}^{\boldsymbol{T}}\right| < \delta\ .\forall j \in Set\}$;

14-**end while**

15-**end if**

16- $\Omega = \{ i \in Set^c \, || \boldsymbol{eigvec}\, \boldsymbol{h}_i^H . \boldsymbol{eigvec}\, \boldsymbol{h}_j | + \boldsymbol{\beta} | \tilde{\boldsymbol{h}}_i^H \tilde{\boldsymbol{h}}_{pu}^T | < \delta \, . \forall j \in Set \}$;

17- Set=$Set \cup \Omega$ (1);

18- Set^c=O/Set;

19- Ω= Φ;

20- T= 0;

21- g=g+1;

22- end while

23- return Set **.**

Termination of the algorithm1

Assigning Users to Clusters

After selecting the cluster heads, user clustering is performed. All remaining users, except for the cluster heads that have already been selected, must be assigned to one of the clusters related to the chosen cluster heads. User clustering is based on the correlation coefficientı of each user with the selected cluster heads [66]. According to the following relationship, which represents a definition of the correlation coefficient, the maximum value of this coefficient is set to 1. Assigning *m*-th user to cluster $\tilde{g}$ in such a way that the following relationship holds:

$$\tilde{g} = \arg\max_{g} \frac{\left| \boldsymbol{eigvec}\, \boldsymbol{h}_{\boldsymbol{m}}^{\boldsymbol{H}} . \boldsymbol{eigvec}\, \boldsymbol{h}_{\boldsymbol{set}(\boldsymbol{g})} \right|}{\| \boldsymbol{eigvec}\, \boldsymbol{h}_{\boldsymbol{m}} \|_2 \cdot \left\| \boldsymbol{igvec}\, \boldsymbol{h}_{\boldsymbol{set}(\boldsymbol{g})} \right\|_2} \qquad (36\text{-}3)$$

$g \in \{1.2.. \cdots . G\}$

According to equation (36-3), for clustering users, correlation coefficients of the desired user channel *m*, who is not a member of Set, with each of the sub-clusters selected in the previous stage are separately calculated. Following this approach, all users present in a specific cluster will have high channel correlation coefficients with each other, while on the other hand, users in other clusters will have lower channel correlation coefficients with each other. Therefore, this method efficiently helps eliminate interference signals between clusters. According to this equation, the user channel cluster matrix is computed using the calculated channel eigenvalues. This user clustering method based on channel correlation coefficients has been a very common approach that does not consider the system's state. It is commonly used for clustering users in various system models. The graphs and simulation results of this method will also be thoroughly examined in Chapter Four.

3-3 Third Proposed Method

Modified ZF beamforming with zero-forcing in the beamforming direction towards the primary user (Null Method).

After clustering users and before sending signals for each cluster according to the OMA scheme, initially, digital precoding operation using the BF matrix on symbols of each cluster is applied.

Following this, according to equation (3-3), the transmitter BS sends the signal corresponding to each of the clusters. To eliminate interference signals between clusters, focusing on the sub-cluster with the strongest user in each cluster, digital precoding at the base station is performed using the beamforming with zero-forcing method [63]. In the ZF method, the transmission beams from the transmitting antennas of the BS are focused on users within each cluster that have the best channel conditions. As a result, the interference effect on other users is almost minimized to zero to prevent interference with the primary user. Since the system model of this paper is based on cognitive radio networks and the primary user in this network is of particular importance, we modify the beamforming in the ZF method and introduce a zero-forcing beamforming approach aligned with the primary user in a downlink communication as the third proposed method.

This method is similar to the ZF method, with the difference that we employ the initial user information in ZF planning in cognitive radio networks. In defining the BF vector, we exactly place the PU channel vector in the last column of the channel vector. By doing this on the PU efficiency, it will have a very positive impact. The reason for this is that when the BF vector is directed towards PU, practically no interference from SUs will affect PU. It is true that by implementing this method, the efficiency of secondary users will slightly decrease, which is acceptable, but interference directed towards the primary user (null method) will be significantly reduced. The impact of this method on PU in low interference thresholds injected from the base station to the network is highly noticeable, and by implementing this method, the achievable information rate for the primary user will greatly improve.

In this context, it is assumed that the best channel conditions for the primary user pu_g located in the specific cluster g are achievable. In other words, due to having the best channel conditions, this user (the primary user) is selected as the primary user for cluster g. Therefore, based on the channel vectors of strong users (cluster heads) in the G cluster, the aggregation matrix associated with millimeter wave MIMO communication channels is defined as follows:

$$\boldsymbol{H1} = \left[\boldsymbol{h}_{m_1}.\boldsymbol{h}_{m_2}.\cdots.\widetilde{\boldsymbol{h}}_{pu}^{T}\right] \tag{37-3}$$

In general, and according to equation (3-37), the matrix forming method in this approach forms the pseudo-inverse matrix of the user channel aggregation matrix at the base station. Therefore, the digital pre-encoding matrix $\bar{\boldsymbol{D}} \in C^{N\times G}$ will be equivalent to the pseudo-inverse of the system MIMO channel aggregation matrix [64]:

$$\overline{\boldsymbol{D1}} = \boldsymbol{H1}(\boldsymbol{H1}^{\boldsymbol{H}}\boldsymbol{H1})^{-\boldsymbol{1}} = \left[\bar{\boldsymbol{d}}_1.\bar{\boldsymbol{d}}_1.\cdots.\bar{\boldsymbol{d}}_G\right] \tag{38-3}$$

In equation (3-38), the vector representing the pre-encoding of digital cluster g is denoted by g, where the normalized version of this vector is calculated as follows:

$$\boldsymbol{d_g} = \frac{\bar{\boldsymbol{d}}_{\boldsymbol{g}}}{\left\|\bar{\boldsymbol{d}}_{\boldsymbol{g}}\right\|_2^2} \tag{39-3}$$

The parameter $\boldsymbol{d_g}$in equation (3-39) is the column g of the digital pre-encoding matrix introduced in equation (1-3).

4- Results and Analysis

4-1 Introduction

In the previous chapter, we thoroughly discussed the system model and its mathematical relationships. By employing several simplifications, we transformed the non-convex problem into a convex optimization problem. Due to the complex nature of convex optimization problems, we will analyze and decompose it using the CVX toolbox in the MATLAB simulation software. The CVX toolbox provides highly practical solvers suitable for solving complex and standard convex optimization problems. In light of the aforementioned discussions, this chapter will focus on analyzing and interpreting the simulation results of the proposed methods in the form of comparative graphs.

4-2 Numerical Parameters Used in Simulation

Before conducting the simulation, this section introduces the input parameters of the problem, which are defined as a set of parameters with specific values in the MATLAB environment. The values of these parameters should be reasonably defined to ensure the practical efficiency of modern communication systems is not compromised. To this end, we initially address the generation of random communication channels and, in a tabular format, determine the numerical values of the input parameters for optimization problem analysis and simulation in the MATLAB software.

The frequency of transmitted signals in fifth-generation telecommunication systems is very high. Since the proposed system model in this paper is based on 5G, the frequency ranges from 30 to 40 GHz. As mentioned in Chapter 3, we define a telecommunication channel as a random channel with millimeter wave MIMO, whose size and phase have statistically Rayleigh and uniform probability distributions, respectively. The telecommunication channel exhibits flat fading and only considers the small-scale fading effect within it. According to reference [66], $\alpha_{g.m}^{(l)}$is a random variable representing the channel coefficient through which each receiver receives the transmitted signal along that path. Statistically, for both direct and non-direct paths, they have different probability distributions. Therefore, the assumption is that there exists one direct path and two non-direct paths among the possible paths for signal reception. The reason for considering only two non-direct paths is that in millimeter-wave communication systems, the transmission frequency is very high, typically in the range of several tens of gigahertz, causing significant signal attenuation in Non-Line-of-Sight (NLoS) paths, hence the effective number of non-direct paths is not significant. Statistically, $\alpha_{g.m}^{(l)}$ follows Complex Gaussian distribution $\mathcal{CN}(0.1)$ in the direct path and a Complex Gaussian distribution $\mathcal{CN}(0.10^{-1})$ in both non-direct paths.

The $\varphi_{g.m}^{(l)}$is a random variable and considered as azimuth angle of departure of the BS transmitter antenna array. Statistically, $\varphi_{g.m}^{(l)}$ has a uniform distribution of $\mathcal{U}(-\pi.\pi)$. According to reference [58], the horizontal distance of each transmitter antenna (d) from each other is considered equal to half the wavelength of the transmitted signal. The numerical values of the input parameters of the optimization problem for analysis and simulation in MATLAB software are given in Table 1-4

Table 4-1 Numerical Values of Simulation Parameters.

Parameter	Description	Numerical value
N	The number of antennas at the transmitter base station	**64**
U	Number of single antenna secondary users	**24**
$L_{g.m}$	The possible paths for receiving the transmitted signal by each primary and secondary receiver	**3**
G	The number of clusters	**4**
I_{th}	Interference threshold determined from the primary user side	**-60 dB w**
SNR	Signal-to-noise ratio	**10dB**
σ_v^2	The received noise power in the antenna of each receiver	**-50 dB w**
P_{max}	The maximum transmit power from the base station transmitter.	$\sigma_v^2 \times (10)^{\frac{SNR}{10}}$
β	The impact factor of the primary user in selecting the cluster head in clustering discussion	**0.5**
α	The scaling factor of NOMA power for users within each cluster	**10**
$Iteration$	The number of occurrences of random telecommunication channel realizations or channel state changes.	**100**
$Counter$	The number of iterations required for the convergence of the CVX solver algorithm to the optimal point in the optimization problem.	**10**

4-3 Analysis of Simulation Results

All simulations were conducted using version R2015a of the MATLAB software on a computer system with the following specifications.

Table 4-2: Complete specifications of the computer system used for conducting the simulations.

Manufacturer	ASUSTeK Computer Inc
Windows Edition	Windows 10 Enterprise
Processor	Intel® – Core™ i7-6700K – CPU@ 4.00 GHz

RAM	32.0 GB
System Type	64-bit Operating System , x64-based Processor

4-3-1 Performance Results of Power Management with Interference Threshold in CRMN System

By extending the convex optimization problem in the radio cognitive domain and adding the interference threshold constraint under the optimized sub-problem as discussed in the previous chapter, the optimization problem in $\boldsymbol{P_4}$ form was obtained.

$$C_4^{(p_3)}: \sum_{g=1}^{G} [\|\boldsymbol{h_{pu}} \boldsymbol{d_g}\|_2^2 \sum_{m=1}^{N_g} p_{g.m}] \leq I_{th} \quad . \quad \forall g.m \tag{1-4}$$

In equation (1-4), the interference threshold $I_{th}$is defined by the primary user. By defining this threshold, a significant amount of incoming interference to the primary user will be prevented; because the base station manages the power to satisfy the I_{th}threshold and the interference constraint, and the user equipment, based on having favorable conditions in its channel, will receive the signal with minimal interference at the receiver. The range of changes in the interference threshold is between $10^{-10}$and 10^{-6}.

PRO1 graph represents the first proposed method in this research. In this method, due to the paper topic, the energy harvesting process and SWIPT reference [66] were not considered, and the cognitive radio interference constraint (1-4) was introduced into the problem. ORG [66] illustrates the reference graph [66].

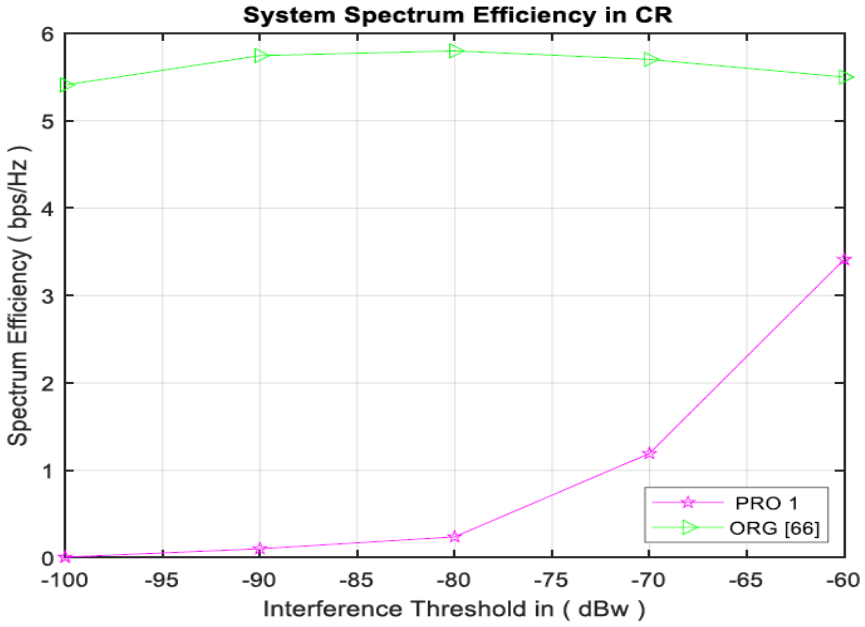

Fig 4-1: Comparison of the spectral efficiency curve obtained as a function of the interference threshold and the reference [66].

By generalizing the problem and bringing it into the cognitive radio domain, as evident in the graphs, the system efficiency decreases significantly due to the presence of the limiting power factor, which is the interference constraint. Additionally, as we utilize zero-forcing beam-forming in shaping the beam, the decrease in system efficiency, especially at low interference thresholds, will be more pronounced, and the impact of the interference constraint will decrease involuntarily with an increase in the threshold. We acknowledge the reduced system throughput compared to the reference [66] because our network is a cognitive radio network, and to prevent incoming interferences to the primary user, it is necessary to define an interference threshold so that the primary user can receive its signal without interference in their receivers. However, the decrease in spectral efficiency of the system, especially at low thresholds, leads to a loss of significant data rates. Therefore, in the proposed methods discussed later, our aim is to enhance the spectral efficiency of the system as much as possible.

4-3-2 Results of Cluster Head Selection Considering the Initial User Status

The cognitive radio network in this paper is composed of several secondary users and one primary user. Therefore, it is important not to select users who are in the vicinity of the primary user and meet the cluster heading conditions as cluster heads, in order to minimize the impact on PU. As mentioned in Algorithm 1 and also alluded to in Chapter 3, we consider the presence of PU in the correlation relationship among cluster head channel and other cognitive users. By doing so, when calculating the correlation of users with cluster heads, the influence of other cognitive users on PU is reduced. In the simulations, we utilized zero-forcing precoding during beam-forming. Now, we aim to investigate the impact of Algorithm 1 on the performance and behavior of the system from various aspects; hence, we consider the interference constraint of cognitive radio for all graphs, and compare this proposed method with three graphs that will be introduced subsequently. It is worth mentioning that at each stage of the proposed methods, the influence of the previous proposed method is taken into account in the simulation process.

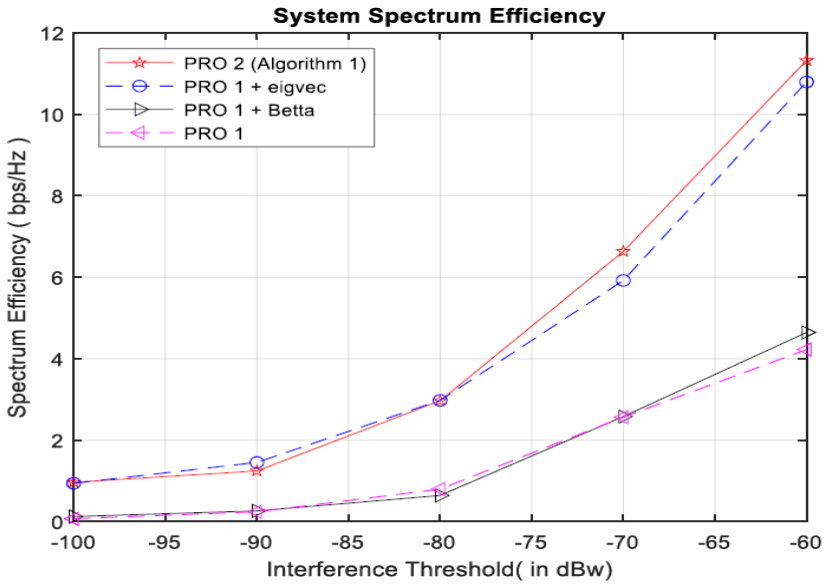

Fig. 4-2: compares the spectral efficiency curve obtained as a function of the interference threshold in the reference method [66] for selecting the cluster head with our proposed new method to prevent neighboring users of the initial user from being selected as the cluster head.

The PRO1 chart is an identifier of the first proposed method. In this section, our attempt is to explain in detail the steps of adding sub-steps to the first proposed method and reaching the second proposed method, which is Algorithm 1.

Step 1: In this stage, as mentioned above, in the cluster head selection section, attention is paid to the problem of neighboring users of the initial user in a way that these users are not selected as cluster heads. According to Fig. 4-2 of PRO1+ Betta, a diagram is presented considering the correlation between cluster heads and other remaining users, where $\beta = 0.5$. As clearly shown in the Fig., at low interference thresholds, due to channels not being in a favorable state and being weak channels, the signal-to-noise ratio, plus interference, is low, and the use of the zero-forcing criterion has reinforced channel noise in these thresholds; thus, the presence of noise and interference causes an undesirable effect on the initial user's channel. Therefore, in these thresholds where the dB is less than -70 in both diagrams, the spectral efficiency curve decreases, and with an increase in the interference threshold (>-70 dB), the spectral efficiency curve gradually ascends, meaning that the interference constraint considered becomes less effective. Consequently, the achievable information rate for users increases, which is logically justifiable based on the explanations provided.

Step 2: In this stage, the problem of assigning users to each cluster is calculated considering the correlation coefficient between the eigenvector corresponding to the largest eigenvalue of the correlation matrix and the channel correlation of each user with the desired cluster head. The graph (PRO1+eigvec), as shown in Fig. 4-2, illustrates the significant impact of this step on improving the spectral efficiency of the proposed method.

Step 3: The second proposed method in this paper, presented as Algorithm 1, is added to the first proposed method. PRO2 also represents the graph of this proposed method. By comparing the first and second proposed methods, it is observed that the addition of Algorithm 1 results in a doubling of the spectral efficiency of the system at low thresholds and an almost threefold growth at high thresholds. Therefore, the outcome of this method compared to the previous one is very promising. However, the issue of low capacity has not been fully resolved, especially at low thresholds, as in both the first and second methods, zero-forcing beam-forming criterion has been employed. ZF intensifies noise at low thresholds (weaker channels), significantly reducing network information rate and causing the system capacity to be lost in these thresholds.

Fig. 4-3 illustrates the spectral efficiency curve of the system in the second proposed method based on a fixed number of 24 users and a variable number of clusters from 4 clusters to 10 clusters with a step length of 1. It is evident that as the number of clusters increases, users are distributed among all clusters, making the clusters more vacant. This phenomenon indicates the same effect as beam-forming, as with an increasing number of clusters, more beams are formed, and if previously only one of the busy clusters benefited well from a narrow beam, here members of other clusters will also benefit more from these beams. Fig. 4-3 indicates that the trend of the system's spectral efficiency curve is almost linearly increasing; therefore, as clusters become more vacant, intra-cluster interference due to NOMA design decreases, leading to an increase in achievable information rate and the signal-to-noise-plus-interference ratio.

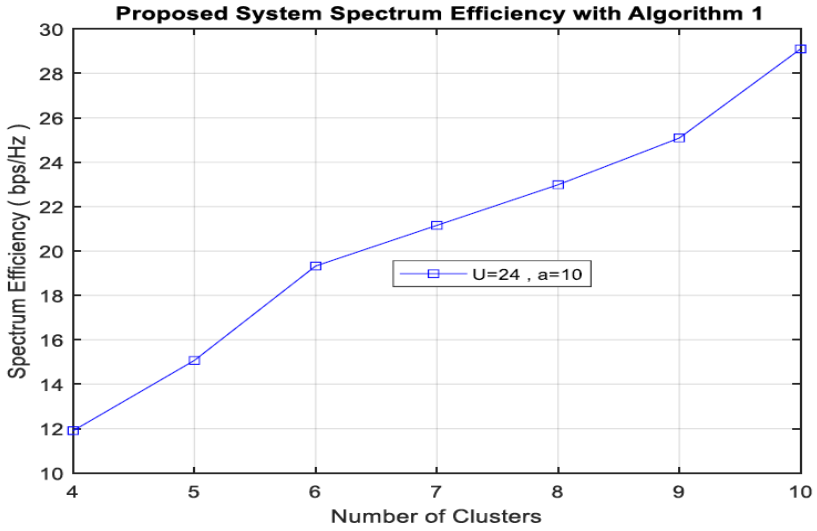

Fig. 4-3: The spectral efficiency curve of the system in accordance with the second proposed method as a function of varying the number of clusters with a fixed number of users.

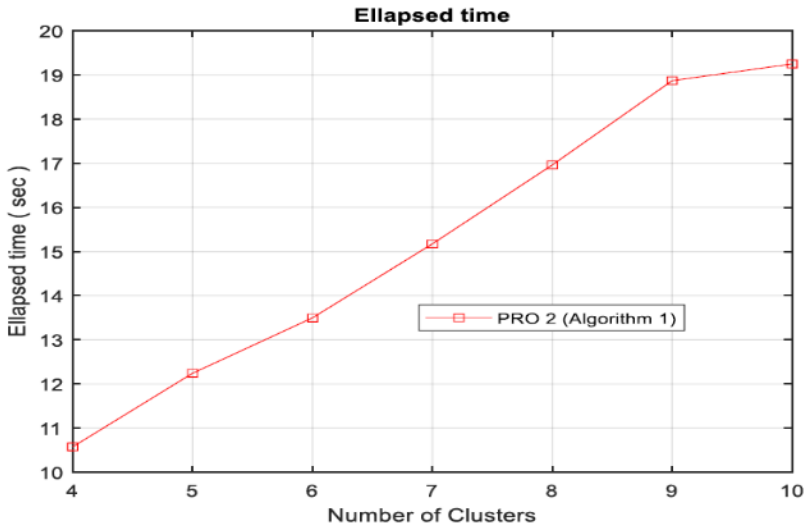

Fig. 4-4: The elapsed time graph of the processor in a computer system for performing computations and solving mathematical problems in the second proposed method based on the increase in complexity in the structure of the telecommunication system.

In Fig. 4-4, we depict the duration it takes for a computer system processor to address a problem in terms of the number of variable clusters. As evident, with an increase in the number of clusters, the complexity of computations and mathematical analysis at the base station (BS) transmitter increases. This issue is justified in a way that as the number of clusters increases, during beam-forming, the number of antenna array elements at the transmitter also increases, thus making the calculation of inverse matrices used in beam-forming based on the zero-forcing criterion more complicated. As shown in Figs. 4-3 and 4-4, it is clear that we have considered the same horizontal axis range for both plots to evaluate the time spent on necessary mathematical analyses for increasing computational complexity based on the change in the number of clusters. According to Fig. 4-3, as the computational complexity increases, the spectral efficiency curve is almost 2.5 times greater, In Fig. 4-4, as the

computational complexity increases, the duration spent has approximately doubled. Beyond a certain point, the trend of curve changes remains relatively constant. Through this method, in a time period that is almost twice as long, we achieve a spectral efficiency nearly 2.5 times greater in the system.

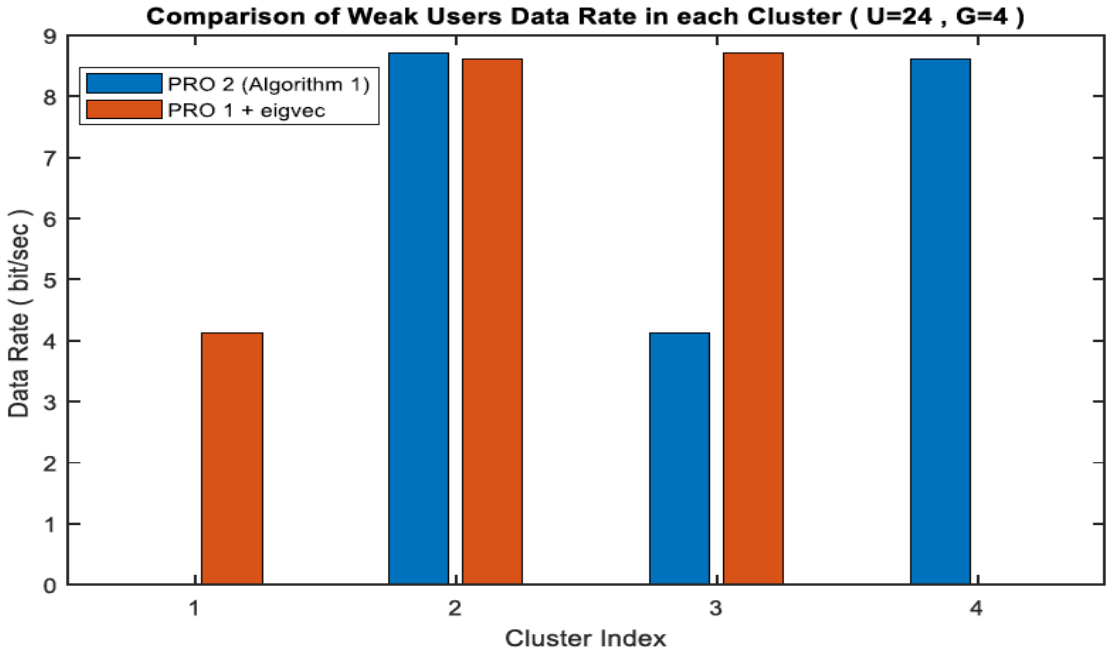

Fig. 4-5: the trend charts of attainable information rates for the weakest user in each cluster in the second proposed method at the interference threshold of -60 dB

The bar graph Fig. 4-5 presents a comparative analysis of achievable information rates for the weakest user in each cluster under the second proposed method at an interference threshold of -60 dB. The blue bar graph represents the second proposed method, while the orange bar graph illustrates this method without considering the effect of the primary user in cluster selection. Simulation of this aspect has been conducted to demonstrate the impact of the third constraint in our proposed method optimization. This constraint pertains to the influence of the power scaling factor of NOMA allocation on cluster users for fairness considerations. The simulation was run for 4 clusters and 24 users. As evident in Fig. 4-5, in both bar graphs, at high interference thresholds, the weakest users in each of the 4 clusters achieve significantly noticeable information rates. This implies that even if no attention is given to the users surrounding the primary user in cluster head selection (orange bar graph), and a cluster head is chosen from among them, it does not affect power allocation to weaker users, ensuring fairness. This means that not only is fairness not violated by this approach, but more power is allocated to the weaker users in each cluster, resulting in improved achievable information rates for these users.

4-3-3 Modified ZF-based Beamforming Results by Introducing Zero in Beamforming towards the Primary User

In the previous section, we have extensively explained this method; therefore, here we refrain from repeating it and directly delve into analyzing the results obtained from the diagrams using this approach.

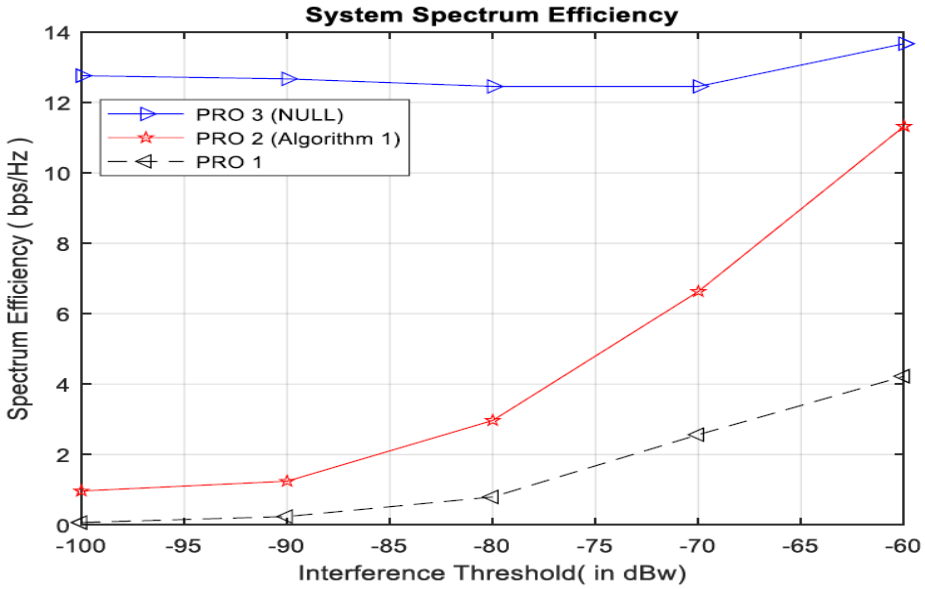

Fig. 4-6: The spectral efficiency curves of all three proposed methods as a function of the interference threshold.

Fig. 4-6 illustrates the simulations conducted in all three proposed methods of this paper. The diagram (PRO3(NULL)) represents the chart resulting from the simulation of the proposed third method. As mentioned earlier, as it is obvious from the diagrams, the weaknesses of the first and second proposed methods are significantly reduced in the efficiency spectrum chart. Consequently, there is a decrease in the capacity at low interference thresholds. As illustrated in Fig. 4-6, in the second proposed method, the weaknesses of the first method were somewhat improved, but these weaknesses were not completely rectified at low thresholds. With the proposal of the third method, the spectral efficiency graph of the system at thresholds below -70 dB will significantly improve compared to higher thresholds. Therefore, in this method, we attempted to prevent capacity reduction at lower interference thresholds and enhance our simulation results noticeably. Utilizing this method involves adding the primary user channel in the last column of the channel matrix. This action leads to narrowing the beam and orienting the antenna array towards the primary user, assuming that the base station knows the status information of the primary user channel. As a result, the base station behaves like the cluster head towards the primary user, enabling the user to receive a good beam and recognize a better channel status compared to other users. By implementing this method, the interference constraint added to the primary user to prevent interference from cognitive users becomes significantly less effective. This is why the graph of this method remains almost constant. This method prevents interference on the primary user side, compensates for the decrease in achievable information rate and capacity at lower thresholds, and weakens the influence of secondary users to the extent that there is no longer a need to impose restrictions on the transmit power. Therefore, with this method, we will conclude that not considering the neighboring users of the primary user as cluster heads using the ZF criterion does not lead us to the desired outcome of zero beam-forming alignment towards the primary user. Hence, the use of the third proposed method for enhancing spectral efficiency, total rate, and system capacity, especially for the primary user, is highly recommended.

The conditions for implementing simulations and all parameters of this method are similar to the second proposed method. With this approach, the trend of changes in the efficiency curve spectrum increases linearly with an increase in the number of clusters. By comparing Figs. 4-3 and 4-7, the trend of changes in the 4-7 curve had more than approximately twice the growth.

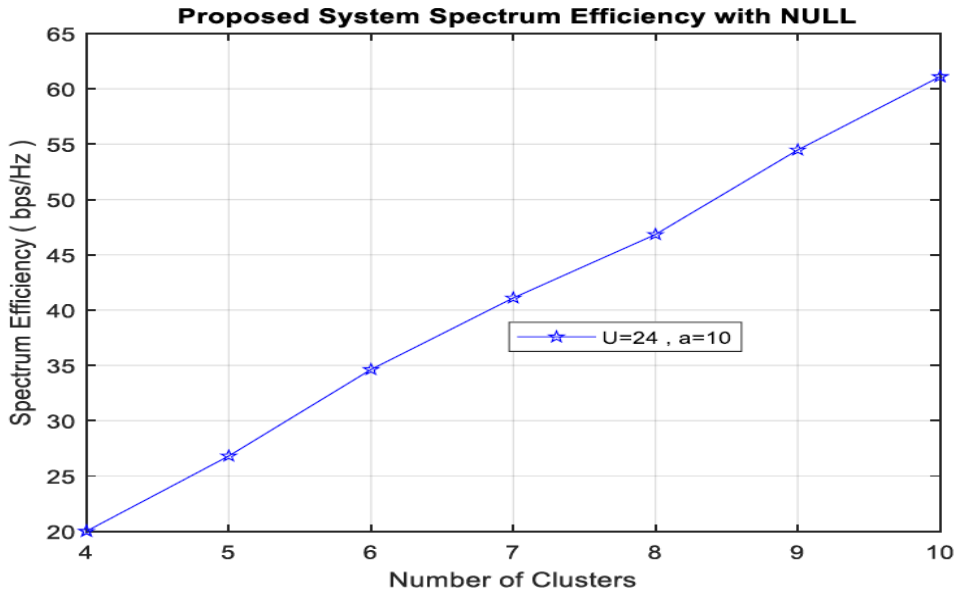

Fig. 4-7: The spectral efficiency curve of the system in accordance with the third proposed method based on varying the number of clusters with a fixed number of users.

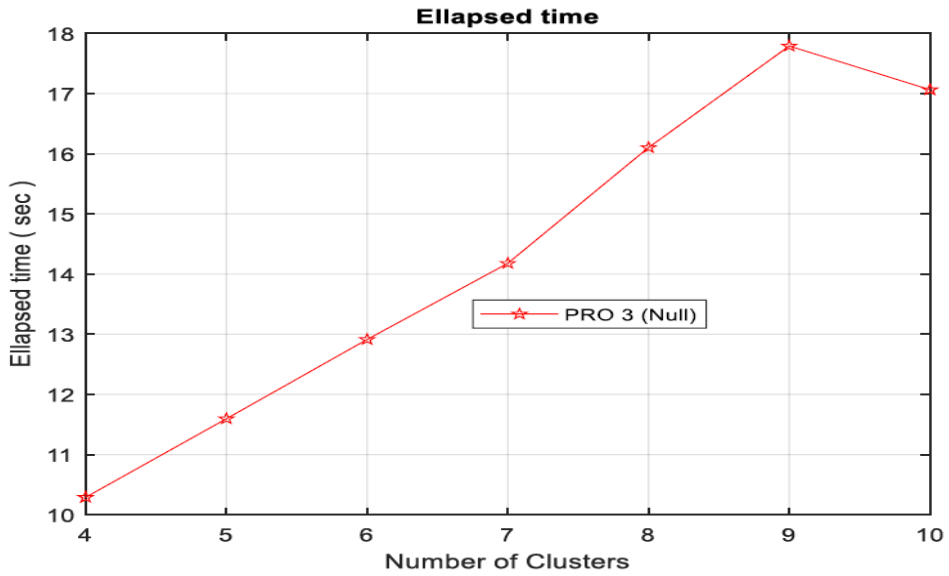

Fig. 4-8: The elapsed time diagram by the computer system processor for performing computations and solving mathematical problems based on the modified ZF in terms of increasing complexity in the telecommunications system structure.

In accordance with Fig. 4-7, with increasing complexity of mathematical computations, the spectral efficiency curve has nearly tripled. As depicted in Fig. 4-8, with further complexity in mathematical computations, the time taken has increased to slightly less than approximately twice and from a certain

point onwards, the trend of time reduction has significantly decreased. Hence, by comparing Fig. 4-4 and 4-8, it is observed that the third method is worthwhile as it can achieve a better spectral efficiency (almost triple) in the system within a time frame almost similar to the previous method.

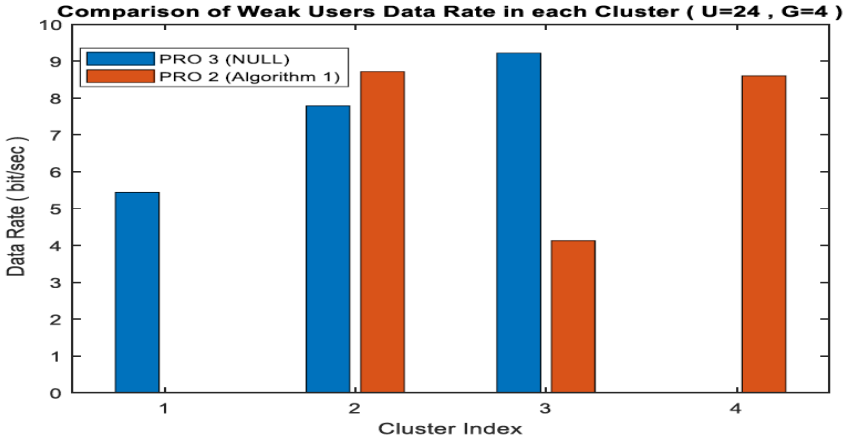

Fig. 4-9: A bar chart comparing the achievable information rates for the weakest user in each cluster in the second and third proposed methods.

Fig. 4-9 provides a comparative analysis of the achievable information rate for the weakest users within each cluster between the second and third proposed methods. The orange bar indicator represents the second proposed method, while the blue bar indicator depicts the third proposed method. As mentioned in the bar chart analysis in Fig. 4-5, the purpose of simulating this Fig. is to demonstrate the impact of the third constraint in the optimization problem to ensure fairness in the NOMA scheme in our proposed methods. This simulation, similar to the previous method, was conducted for 4 clusters and 24 users. As evident in Fig. 4-9, in both methods, the weakest users in each cluster have achieved a considerable information rate. Therefore, our proposed methods not only do not violate the nature of NOMA technology based on ensuring fairness and proper implementation of SIC but also provide weaker users in each cluster with more capacity. Consequently, SIC operates correctly, and as a result, the achievable information rate for each user also improves.

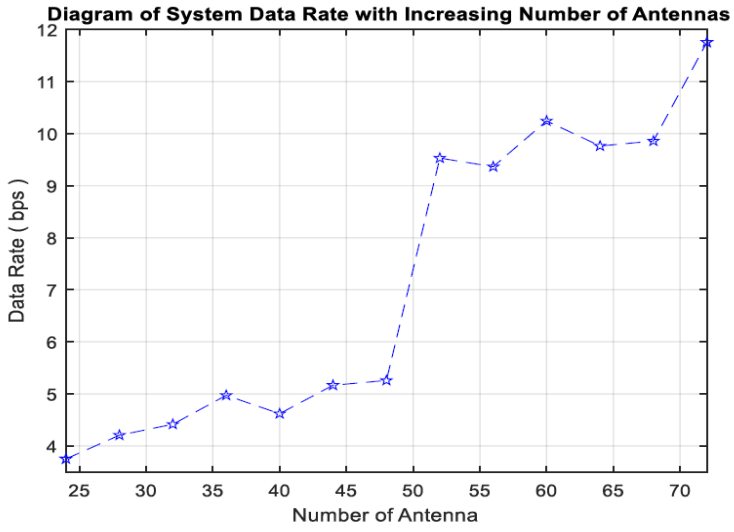

Fig. 4-10: The system information rate with respect to the increase in the number of antennas.

Fig. 4-10 illustrates the evolution of the achievable data rate for users in a massive MIMO system (CRMN). As the number of antennas increases, antenna gain rises, signals are received more strongly, the data rate of received signals improves, and the system exhibits scalability properties. However, at a certain point, the data rate curve does not increase significantly as the number of antennas grows and the beams sharpen because some users within NOMA lose coverage.

.5- Conclusion

The optimization problem concerning the CRMN system aiming to maximize the sum user rate network has been formulated. This problem includes an objective function and several constraints, where the objective function is non-convex and the constraints of the problem are all linear and convex. Therefore, the formulated optimization problem is also non-convex. By employing simplifications and several lemmas, the problem was transformed into the form of a convex optimization problem. The convexities form of the problem was then analyzed and deconstructed using the CVX toolbox in the MATLAB computational simulation software. The optimization variables $\{p_{g.m}g\}$ were optimized using the CVX toolbox. In the analysis of simulation results based on our proposed methods, which involve power management in the CRMN network by introducing interference constraints from the primary user side, cluster selection considering the status of the primary user, and beamforming based on modified ZF, we have demonstrated that by generalizing the problem to a cognitive radio problem and adding interference constraints, the efficiency graph decreases compared to a problem without interference constraints, which is intuitive. While presenting a second proposed method, although the efficiency graph showed significant improvement in a spectral domain, at low interference thresholds, the information rate and throughput remained low. Consequently, at these low interference thresholds, we were unable to achieve a good network capacity. Ultimately, utilizing a third method, the issue of reduced information rate and spectral efficiency of the system at low thresholds noticeably improved. However, a crucial point found in the analysis of the graphs is that the simultaneous use of NOMA and massive MIMO technology in a network up to a certain stage enhances the overall system rate. Excessive increase in antennas not only fails to enhance network capacity but also leads to the exclusion of some users within the NOMA scheme, exacerbating the system's capacity reduction.

REFERENCES

[1] F. Zhou, Y. Wu, Y.-C. Liang, Z. Li, Y. Wang, and K.-K. Wong, "State of the art, taxonomy, and open issues on cognitive radio networks with NOMA," *IEEE Wireless Communications*, vol. 25, no. 2, pp. 100-108, 2018.

[2] H. Shahrokh and K. Mohamed-pour, "Sub-optimal power allocation in MIMO-OFDM based cognitive radio networks," in *2010 6th International Conference on Wireless Communications Networking and Mobile Computing (WiCOM)*, 2010: IEEE, pp. 1-5.

[3] B. Wang and K. R. Liu, "Advances in cognitive radio networks: A survey," *IEEE Journal of selected topics in signal processing*, vol. 5, no. 1, pp. 5-23, 2010.

[4] S. K. Sharma, T. E. Bogale, S. Chatzinotas, B. Ottersten, L. B. Le, and X. Wang, "Cognitive radio techniques under practical imperfections: A survey," *IEEE Communications Surveys & Tutorials*, vol. 17, no. 4, pp. 1858-1884, 2015.

[5] K. Senel, H. V. Cheng, E. Björnson, and E. G. Larsson, "What role can NOMA play in massive MIMO?," *IEEE Journal of Selected Topics in Signal Processing,* vol. 13, no. 3, pp. 597-611, 2019.

[6] I. F. Akyildiz, W.-Y. Lee, M. C. Vuran, and S. Mohanty, "NeXt generation/dynamic spectrum access/cognitive radio wireless networks: A survey," *Computer networks,* vol. 50, no. 13, pp. 2127-2159, 2006.

[7] A. Goldsmith, S. A. Jafar, I. Maric, and S. Srinivasa, "Breaking spectrum gridlock with cognitive radios: An information theoretic perspective," *Proceedings of the IEEE,* vol. 97, no. 5, pp. 894-914, 2009.

[8] Y. Tao, L. Liu, S. Liu, and Z. Zhang, "A survey: Several technologies of non-orthogonal transmission for 5G," *China communications,* vol. 12, no. 10, pp. 1-15, 2015.

[9] E. Z. Tragos, S. Zeadally, A. G. Fragkiadakis, and V. A. Siris, "Spectrum assignment in cognitive radio networks: A comprehensive survey," *IEEE Communications Surveys & Tutorials,* vol. 15, no. 3, pp. 1108-1135, 2013.

[10] G. I. Tsiropoulos, O. A. Dobre, M. H. Ahmed, and K. E. Baddour, "Radio resource allocation techniques for efficient spectrum access in cognitive radio networks," *IEEE Communications Surveys & Tutorials,* vol. 18, no. 1, pp. 824-847, 2014.

[11] A. Ahhmadfard, A. Jamshidi, and M. Biguesh, "Capacity and power allocation for spectrum sharing in cognitive radio systems under unknown channel state information and imperfect spectrum sensing," *IET communications,* vol. 6, no. 15, pp. 2387-2394, 2012.

[12] A. Kaushik, S. K. Sharma, S. Chatzinotas, B. Ottersten, and F. Jondral, "Estimation-Throughput tradeoff for underlay cognitive radio systems," in *2015 IEEE International Conference on Communications (ICC),* 2015: IEEE, pp. 7701-7706.

[13] K. Higuchi and A. Benjebbour, "Non-orthogonal multiple access (NOMA) with successive interference cancellation for future radio access," *IEICE Transactions on Communications,* vol. 98, no. 3, pp. 403-414, 2015.

[14] L. B. Le and E. Hossain, "Resource allocation for spectrum underlay in cognitive radio networks," *IEEE Transactions on Wireless communications,* vol. 7, no. 12, pp. 5306-5315, 2008.

[15] D. Cabric, I. D. O'Donnell, M.-W. Chen, and R. W. Brodersen, "Spectrum sharing radios," *IEEE Circuits and Systems Magazine,* vol. 6, no. 2, pp. 30-45, 2006.

[16] S. Srinivasa and S. A. Jafar, "Cognitive radios for dynamic spectrum access-the throughput potential of cognitive radio: A theoretical perspective," *IEEE communications Magazine,* vol. 45, no. 5, pp. 73-79, 2007.

[17] M. Naeem, A. Anpalagan, M. Jaseemuddin, and D. C. Lee, "Resource allocation techniques in cooperative cognitive radio networks," *IEEE Communications surveys & tutorials,* vol. 16, no. 2, pp. 729-744, 2013.

[18] H. S. Shahraki, K. Mohamed-Pour, and L. Vangelista, "Efficient resource allocation for MIMO-OFDMA based cognitive radio networks," in *2011 Wireless Telecommunications Symposium (WTS)*, 2011: IEEE, pp. 1-6.

[19] X. Liu, Y. Liu, X. Wang, and H. Lin, "Highly efficient 3-D resource allocation techniques in 5G for NOMA-enabled massive MIMO and relaying systems," *IEEE Journal on Selected Areas in Communications*, vol. 35, no. 12, pp. 2785-2797, 2017.

[20] Y. Chen *et al.*, "Toward the standardization of non-orthogonal multiple access for next generation wireless networks," *IEEE Communications Magazine*, vol. 56, no. 3, pp. 19-27, 2018.

[21] M. Mohammadi *et al.*, "Full-duplex non-orthogonal multiple access for next generation wireless systems," *IEEE Communications Magazine*, vol. 57, no. 5, pp. 110-116, 2019.

[22] L. Dai, B. Wang, Y. Yuan, S. Han, I. Chih-Lin, and Z. Wang, "Non-orthogonal multiple access for 5G: solutions, challenges, opportunities, and future research trends," *IEEE Communications Magazine*, vol. 53, no. 9, pp. 74-81, 2015.

[23] S. R. Islam, N. Avazov, O. A. Dobre, and K.-S. Kwak, "Power-domain non-orthogonal multiple access (NOMA) in 5G systems: Potentials and challenges," *IEEE Communications Surveys & Tutorials*, vol. 19, no. 2, pp. 721-742, 2016.

[24] O. Maraqa, A. S. Rajasekaran, S. Al-Ahmadi, H. Yanikomeroglu, and S. M. Sait, "A survey of rate-optimal power domain NOMA with enabling technologies of future wireless networks," *IEEE Communications Surveys & Tutorials*, vol. 22, no. 4, pp. 2192-2235, 2020.

[25] N. Glei and R. B. Chibani, "Power allocation for energy-efficient downlink NOMA systems," in *2019 19th International Conference on Sciences and Techniques of Automatic Control and Computer Engineering (STA)*, 2019: IEEE, pp. 611-613.

[26] Z. Ding *et al.*, "Application of non-orthogonal multiple access in LTE and 5G networks," *IEEE Communications Magazine*, vol. 55, no. 2, pp. 185-191, 2017.

[27] S. Islam, M. Zeng, and O. A. Dobre, "NOMA in 5G systems: Exciting possibilities for enhancing spectral efficiency," *arXiv preprint arXiv:1706.08215*, 2017.

[28] Z. Q. Al-Abbasi and D. K. So, "Power allocation for sum rate maximization in non-orthogonal multiple access system," in *2015 IEEE 26th Annual International Symposium on Personal, Indoor, and Mobile Radio Communications (PIMRC)*, 2015: IEEE, pp. 1649-1653.

[29] T. L. Marzetta and H. Q. Ngo, *Fundamentals of massive MIMO*. Cambridge University Press, 2016.

[30] V. Tarokh, N. Seshadri, and A. R. Calderbank, "Space-time codes for high data rate wireless communication: Performance criterion and code construction," *IEEE transactions on information theory*, vol. 44, no. 2, pp. 744-765, 1998.

[31] Z. Ding, F. Adachi, and H. V. Poor, "The application of MIMO to non-orthogonal multiple access," *IEEE transactions on wireless communications*, vol. 15, no. 1, pp. 537-552, 2015.

[32] X. Li, J. Li, Y. Liu, Z. Ding, and A. Nallanathan, "Outage performance of cooperative NOMA networks with hardware impairments," in *2018 IEEE Global Communications Conference (GLOBECOM)*, 2018: IEEE, pp. 1-6.

[33] Z. Chen, Z. Ding, X. Dai, and G. K. Karagiannidis, "On the application of quasi-degradation to MISO-NOMA downlink," *IEEE Transactions on Signal Processing*, vol. 64, no. 23, pp. 6174-6189, 2016.

[34] M. El Tanab and W. Hamouda, "Resource allocation for underlay cognitive radio networks: A survey," *IEEE Communications Surveys & Tutorials*, vol. 19, no. 2, pp. 1249-1276, 2016.

[35] J. G. Proakis, "Spread spectrum signals for digital communications," *Wiley Encyclopedia of Telecommunications*, 2003.

[36] Y. Yang, G. Scutari, P. Song, and D. P. Palomar, "Robust MIMO cognitive radio systems under interference temperature constraints," *IEEE Journal on Selected Areas in Communications*, vol. 31, no. 11, pp. 2465-2482, 2013.

[37] M. G. Adian and H. Aghaeinia, "Optimal resource allocation for opportunistic spectrum access in multiple-input multiple-output-orthogonal frequency division multiplexing based cooperative cognitive radio networks," *IET Signal Processing*, vol. 7, no. 7, pp. 549-557, 2013.

[38] Z. Chu, F. Zhou, Z. Zhu, R. Q. Hu, and P. Xiao, "Wireless powered sensor networks for Internet of Things: Maximum throughput and optimal power allocation," *IEEE Internet of Things Journal*, vol. 5, no. 1, pp. 310-321, 2017.

[39] F. Shams, G. Bacci, and M. Luise, "A survey on resource allocation techniques in OFDM (A) networks," *Computer Networks*, vol. 65, pp. 129-150, 2014.

[40] E. Bedeer, O. A. Dobre, M. H. Ahmed, and K. E. Baddour, "Resource allocation for spectrum sharing cognitive radio networks," in *2013 IEEE International Conference on Communications (ICC)*, 2013: IEEE, pp. 2764-2769.

[41] A. Benjebbour, Y. Saito, Y. Kishiyama, A. Li, A. Harada, and T. Nakamura, "Concept and practical considerations of non-orthogonal multiple access (NOMA) for future radio access," in *2013 International Symposium on Intelligent Signal Processing and Communication Systems*, 2013: IEEE, pp. 770-774.

[42] B. Di, S. Bayat, L. Song, and Y. Li, "Radio resource allocation for downlink non-orthogonal multiple access (NOMA) networks using matching theory," in *2015 IEEE global communications conference (GLOBECOM)*, 2015: IEEE, pp. 1-6.

[43] Q. Sun, S. Han, I. Chin-Lin, and Z. Pan, "On the ergodic capacity of MIMO NOMA systems," *IEEE Wireless Communications Letters*, vol. 4, no. 4, pp. 405-408, 2015.

[44] F. M. J. Willems, "Review of 'Elements of Information Theory' (Cover, T.M., and Thomas, J.A.; 1991)," *IEEE Trans. Inf. Theory*, vol. 39, no. 1, pp. 313-, 1993.

[45] M. Zeng, A. Yadav, O. A. Dobre, G. I. Tsiropoulos, and H. V. Poor, "On the sum rate of MIMO-NOMA and MIMO-OMA systems," *IEEE Wireless communications letters*, vol. 6, no. 4, pp. 534-537, 2017.

[46] M. Mohammadi and S. M. H. Andargoli, "Sum throughput maximization for downlink MIMO-OFDMA based cognitive radio networks in spectrum overlay model," in *2016 8th International Symposium on Telecommunications (IST)*, 2016: IEEE, pp. 72-77.

[47] J. Choi, "On the power allocation for a practical multiuser superposition scheme in NOMA systems," *IEEE Communications Letters*, vol. 20, no. 3, pp. 438-441, 2016.

[48] J. Choi, "On the power allocation for MIMO-NOMA systems with layered transmissions," *IEEE transactions on wireless communications*, vol. 15, no. 5, pp. 3226-3237, 2016.

[49] G. J. Foschini, "Layered space-time architecture for wireless communication in a fading environment when using multi-element antennas," *Bell labs technical journal*, vol. 1, no. 2, pp. 41-59, 1996.

[50] G. J. Foschini, D. Chizhik, M. J. Gans, C. Papadias, and R. A. Valenzuela, "Analysis and performance of some basic space-time architectures," *IEEE Journal on Selected areas in communications*, vol. 21, no. 3, pp. 303-320, 2003.

[51] Y. Sun, D. W. K. Ng, and R. Schober, "Resource allocation for MC-NOMA systems with cognitive relaying," in *2017 IEEE Globecom Workshops (GC Wkshps)*, 2017: IEEE, pp. 1-7.

[52] D. Zhang, Y. Liu, Z. Ding, Z. Zhou, A. Nallanathan, and T. Sato, "Performance analysis of non-regenerative massive-MIMO-NOMA relay systems for 5G," *IEEE Transactions on Communications*, vol. 65, no. 11, pp. 4777-4790, 2017.

[53] L. Dai, B. Wang, M. Peng, and S. Chen, "Hybrid precoding-based millimeter-wave massive MIMO-NOMA with simultaneous wireless information and power transfer," *IEEE Journal on Selected Areas in Communications*, vol. 37, no. 1, pp. 131-141, 2018.

[54] Y. S. Xiao and D. H. Tsang, "Interference alignment beamforming and power allocation for cognitive MIMO-NOMA downlink networks," in *2019 IEEE Wireless Communications and Networking Conference (WCNC)*, 2019: IEEE, pp. 1-6.

[55] D.-T. Do and A.-T. L. Chi-Bao Le, "Cooperative underlay cognitive radio assisted NOMA: secondary network improvement and outage performance," *TELKOMNIKA Telecommunication Computing Electronics and Control*, vol. 17, no. 5, pp. 2147-2154, 2019.

[56] D. T. Do, A. T. Le, and B. M. Lee, "NOMA in Cooperative Underlay Cognitive Radio Networks Under Imperfect SIC," *IEEE Access*, vol. 8, pp. 86180-86195, 2020, doi: 10.1109/ACCESS.2020.2992660.

[57] O. El Ayach, S. Rajagopal, S. Abu-Surra, Z. Pi, and R. W. Heath, "Spatially sparse precoding in millimeter wave MIMO systems," *IEEE transactions on wireless communications*, vol. 13, no. 3, pp. 1499-1513, 2014.

[58] X. Gao, L. Dai, S. Han, I. Chih-Lin, and R. W. Heath, "Energy-efficient hybrid analog and digital precoding for mmWave MIMO systems with large antenna arrays," *IEEE Journal on Selected Areas in Communications,* vol. 34, no. 4, pp. 998-1009, 2016.

[59] L. Dai, B. Wang, Z. Ding, Z. Wang, S. Chen, and L. Hanzo, "A survey of non-orthogonal multiple access for 5G," *IEEE communications surveys & tutorials,* vol. 20, no. 3, pp. 2294-2323, 2018.

[60] J. R. Magnus and H. Neudecker, *Matrix differential calculus with applications in statistics and econometrics*. John Wiley & Sons, 2019.

[61] Q. Zhang, Q. Li, and J. Qin, "Robust beamforming for nonorthogonal multiple-access systems in MISO channels," *IEEE Transactions on Vehicular Technology,* vol. 65, no. 12, pp. 10231-10236, 2016.

[62] W. V. Mauricio, D. C. Araujo, F. H. Neto, F. R. Lima, and T. F. Maciel, "A low complexity solution for resource allocation and SDMA grouping in massive MIMO systems," in *2018 15th International Symposium on Wireless Communication Systems (ISWCS)*, 2018: IEEE, pp. 1-6.

[63] B. Wang, L. Dai, Z. Wang, N. Ge, and S. Zhou, "Spectrum and energy-efficient beamspace MIMO-NOMA for millimeter-wave communications using lens antenna array," *IEEE Journal on Selected Areas in Communications,* vol. 35, no. 10, pp. 2370-2382, 2017.

[64] W. Yuan, V. Kalokidou, S. M. Armour, A. Doufexi, and M. A. Beach, "Application of non-orthogonal multiplexing to mmWave multi-user systems," in *2017 IEEE 85th Vehicular Technology Conference (VTC Spring)*, 2017: IEEE, pp. 1-6.